FURTHER DEVELOPMENTS OF THE BOUNDARY ELEMENT METHOD WITH APPLICATIONS IN MINING.

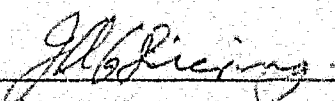Julian Anthony Cameron Diering

A dissertation submitted to the Faculty of Engineering University of the Witwatersrand, Johannesburg for the Degree of Master of Science

Johannesburg 1981.

DECLARATION

I declare that this dissertation is my own, unaided work. It is being submitted for the degree of Master of Science in the University of the Witwatersrand, Johannesburg. It has not been submitted before for any degree or examination in any other University.

Julian Anthony Cameron Diering

3rd day of November ,19 81

ACKNOWLEDGEMENTS

A B S T R A C T

FURTHER DEVELOPMENTS OF THE BOUNDARY ELEMENT METHOD WITH APPLICATIONS IN MINING

DIERING, Julian Anthony Cameron, University of Witwatersrand, 1981.

Three computer programmes designed for the determination of stresses and displacements in and around mine excavations are described. The first is a three-dimensional, boundary element formulation which allows for modelling of large scale non-homogeneities in the rock mass surrounding the mine excavations. In addition, shear or tensile failure of the geological interfaces may be modelled in a realistic manner. The second is a "mixed boundary element" formulation comprising three-dimensional boundary and displacement discontinuity elements into a single programme. The programme enables the interaction of planar or tabular features with open or massive excavations to be modelled efficiently. The third, an extension to an existing programme enables mining in non-homogeneous ground to be modelled in two dimensions using the displacement discontinuity method.

Examples are given demonstrating the applicability of these programmes to mining problems. The programmes will run on most mini computers making them practical design aids readily available to the rock mechanics engineer.

C O N T E N T S

C O N T E N T S (continued)

LIST OF FIGURES

LIST OF FIGURES
(continued)

LIST OF TABLES

LIST OF TABLES
(continued)

CHAPTER 1 INTRODUCTION

1.1 Background

The determination of stresses and displacements in and around mine excavations plays an important role in mine planning and mining rock mechanics. Usually, however, the geology surrounding and the geometry of the mine excavation are so complex that (a) analytic solutions are not available and (b) numerous simplifying assumptions have to be made about the geology and geometry before numerical or, sometimes, analytical solutions may be obtained. The geology of the problem is usually simplified by assumptions such as homogeneity, isotropy and linear elastic material while geometric simplifications include two-dimensional or axisymmetric representation of a fully three-dimensional problem, an assumption of an infinite, finite or semi-infinite region of space and smoothing of excavation surfaces.

The limited applicability of analytic solutions to practical mining problems together with the ready availability of digital computers has resulted in an ever increasing use of computer based stress analysis techniques in mining rock mechanics. Three major classes of numerical stress analysis have emerged, namely the finite difference, finite element and surface element methods.

The finite difference method finds some application in simple time dependent problems but has been largely superceded by the finite element method. This method requires that a sufficiently large volume of material surrounding the mine workings being analysed be divided into volume elements. Simplifying assumptions about the stresses and displacements within an element are made and each element only influences its neighbours. As such, each element may be assigned unique properties so that the finite element method is well suited to the analysis of non-homogeneous or non-linearly elastic problems.

Surface element methods describe a problem in terms of the excavation surfaces, geological interfaces and very often the surrounding ground surface also. These surfaces are divided into surface or boundary elements and their mutual interaction calculated so as to satisfy boundary conditions imposed on the surfaces.

It is immediately apparent that surface area to volume ratio of a problem will determine the relative applicability of a finite or surface element technique. Equally important are the degrees of non-homogeneity and non-linear behaviour involved. Both methods (and in fact most stress analysis formulations) usually assume that the host rock is isotropic. The validity of this assumption in most problems is generally accepted even though numerous rock types are grossly anisotropic. The assumption of isotropy is therefore maintained throughout the rest of this dissertation.

Surface or boundary element methods are based upon the numerical solution of the boundary integral equation (BIE). Different formulations of the BIE include specification of surface tractions and displacements, "fictitious forces" and displacements or surface tractions and displacement discontinuities. The displacement discontinuity formulation forms a special class of boundary element method commonly referred to as the displacement discontinuity method. Distinction is hereafter made between the displacement discontinuity method (DDM) and other boundary element methods (BEM) and the finite element method (FEM).

Just as the FEM and BEM formulations have their relative merits and disadvantages so do the BEM and DDM formulations. To a first degree of approximation it may be said that the DDM is best suited to the modelling of narrow or tabular excavations and their interaction with faults or joints while the BEM is well suited to modelling open excavations with the presence of limited non-homogenities.

1.2 Existing formulations

Cruse (1969) described a boundary element formulation in three

dimensions for homogeneous bodies. Boundary conditions at the surface elements are specified in terms of constant tractions and displacements over triangular elements. Examples are given to demonstrate the applicability of the formulation to fairly simple problems. Evaluation of influence coefficients (the influence of one component of displacement or traction of one element upon another) is done analytically. The main draw back of this formulation is that a large number of elements are required for practical problems.

Cruse (1974) described an improved version in which displacements and tractions are allowed to vary linearly over each surface element. This formulation gives improved accuracy for the same number of surface elements.

A boundary element formulation in which curved elements with linear, quadratic or cubic variation of tractions and displacements is allowed over each element was described by Lachat and Watson (1976). A computer programme was described which is capable of handling a wide range of problems including thin plate problems. The computer programme is very long (about 10 000 lines of Fortran IV) and might not be well suited to run on small mini-computers. A problem which arises when higher order elements are used is that the integration procedures described to date will only work for finite geometries. It is possible that minor modifications to these programmes would enable them to model typical rock mechanics problems, although no literature describing any such modifications was found.

Examples given in the above formulations are related primarily to mechanical engineering and fracture machanics and solution of the equations is carried out using Gaussian Elimination, a technique not well suited to the solution of large systems of linear equations on a small mini-computer.

Deist and Georgiades (1976) described a slightly different approach in which displacements and "fictitious forces" are taken as constant over flat triangular elements. Evaluation of influence coefficients is done numerically and the equations are solved using a stationary

second degree iterative solution technique not unlike successive over relaxation (SOR). This iterative technique offers considerable savings of computation time. Machine time is further reduced by the implementation of a sophisticated "lumping mechanism" whereby groups of elements are treated as single elements when calculating their influences upon other remote elements. Examples are given showing the applicability of this programme to mining rock mechanics problems. The programme assumes a homogeneous rockmass and is also too large to be easily implemented on a mini-computer.

Bannerjie and Butterfield (1977) describe a formulation similar to that of Cruse (1969) and give examples of applications in soil mechanics. None of the above formulations allow for slip or failure to occur at an interface (fault or joint) unless such failure is implemented manually step by step. Hocking (1976) has attempted to implement slip on two-dimensional boundary element interfaces. His approach, however, met with little success: "results should be viewed with suspicion until validation is obtained".

The displacement discontinuity method has found wide application for mining problems involving tabular excavations. Three-dimensional formulations have been described by Salamon (1963, 1964 (a),(b),(c)) and Starfield and Crouch (1973) in which, typically, a planar tabular excavation remote from the earth's surface is divided into a large number of square elements. The relative movement between hangingwall and footwall defines the "displacement discontintuity" which is assumed constant over each element. These formulations cannot model the interaction between tabular excavations and the ground surface or other non-tabular excavations.

Morris (1976) of the Chamber of Mines of South Africa has extended the method for tabular excavations close to but not outcropping at the earth's surface or for a series of parallel tabular excavations. These formulations cannot model outcropping excavations or any inter-action with non-tabular excavations or geological discontinuities as is the case with the programmes described in this dissertation.

Crouch (1976) extended the DDM in two-dimensions to handle excavations of arbitrary shape in a homogeneous rock mass. Failure of faults and joints is realistically modelled by means of a Mohr-Coulomb failure criterion. This very useful extension to the DDM cannot, however, model non-homogeneities.

1.3 Scope of the dissertation

The major portion of this dissertation is concerned with stress analysis formulations in three-dimensions. Numerical and computational problems associated with three-dimensional analyses are in general much greater than for equivalent two-dimensional analyses. Execution times, storage requirements, data preparation times and degrees of freedom are usually an order of magnitude greater than for two-dimensional formulations. As a result, the cost of a three-dimensional stress analysis is usually high and often prohibitive.

One approach used to alleviate the problem centres around the introduction of sophisticated elements. Zienkiewicz (1971) has used sophisticated finite elements to great advantage while Lachat and Watson (1976) and Cruse (1973) have introduced improved boundary elements with equal success. With this approach it is still necessary to solve most problems on large main frame systems.

The approach adopted in this dissertation relies on efficient handling of a large number of simple elements. Reduction of main and disk storage requirements, programme size and execution times were main goals of this dissertation. In particular it was necessary that any formulation be able to run on a small 16- bit mini-computer. Satisfaction of this requirement results in a great cost reduction to those users who have mini-computers but have to rely on commercial computing beureux for three-dimensional problems. A similar approach has been used by Deist and Geordiodes (1976). Much of the experience gained in efficient handling of a large number of simple elements is directly applicable to the more sophisticated boundary elements.

The first formulation described here is based on that of Cruse (1969). He introduced a simple triangular boundary element. Calculation of influence coefficients - the effect of one element on another - is done analytically and the resulting equations are solved using Gaussian elimination with iteration on the residues. His examples are concerned with problems in fracture mechanics. The following changes are made to his formulation:

(i)   Equations are solved iteratively using the method of successive over relaxation.

(ii) Elements are grouped into "lump" elements.

(iii) Non-homogeneous problems may be analysed.

(iv) Slip or failure of interfaces may be modelled by a Mohr-Coulamb failure criterion.

(v)   A variety of symmetry conditions may be imposed.

(vi) The programme will run on a small mini-computer.

The second formulation combines the above boundary element programme with a displacement discontinuity formulation based upon that of Starfield and Crouch (1976). Displacement discontinuity elements are used to model a fault or a tabular excavation while the boundary elements may be used to model the earth's surface, an open pit or a massive excavation. This formulation has significant advantages over the first for many problems.

Finally an improvement to the two-dimensional displacement discontinuity formulation of Crouch (1976) is described here. He described modelling of mining in faulted ground which is homogeneous. The programme MINAP of Crouch is modified here enabling modelling of a large number of non-homogeneous problems.

Examples are given to test the accuracy of the three-dimensional formulations against analytic or other formulations and which demonstrate the applicability of these programmes to practical rock mechanics problems. These include:

(i)   A long rectangular tunnel

(ii) Two massive excavations close to the earth's surface

(iii) Interaction between an underground tabular and open pit excavations

(iv) Tabular excavation mining up to a fault

(v)   Interaction between massive underground and open pit excavations

(vi) A pile socketed in rock with slip on the pile/rock interface.

The three formulations are henceforth referred to by the programme names:

BEM   -   Boundary element method (formulation 1)

MBEM   -   Mixed boundary element method (formulation 2)

MINAPH -   DDM for non-homogeneous problems (formulation 3)

Briefly the contents of the dissertation are as follows:

Chapter 2 gives the basic equations for the BEM and MBEM programmes.

Chapter 3 describes the numerical integration procedures used for evaluating influence coefficients.

Chapter 4 describes the implementation of lumping into the BEM and MBEM programmes. The primary objectives of the lumping mechanism are:

    (i)   to convert a full system of equations into one which is about 20% to 50% populated thus reducing disk storage and execution time,

    (ii) to produce additional checks on input data and

    (iii) to reduce main memory required

Chapter 5 describes the implementation of interface elements and symmetry conditions. When two or more subregions with different elastic properties are being modelled, it is possible to allow the material interface to fail in shear or in tension.

Chapter 6 describes a similar implementation of interface elements into the two-dimensional programme MINAP of Crouch (1976).

This allows for modelling of a wide range of non-homogeneous problems while allowing for possible tensile or shear failure of the material interfaces. The contents of this chapter form the basis of a recent publication Diering (1980a).

Chapter 7 describes programme validation, with a few examples to assess programme accuracy and numerical integration sensitivity.

Chapter 8 gives a brief discussion of some of the programming considerations. Particular attention is given to disk storage and disk access considerations.

Chapter 9 contains various examples demonstrating a wide variety of applications in rock mechanics.

Chapter 10 gives conclusions and a general discussion of the dissertation.

APPENDICES

1 Equivalence of displacement discontinuity and boundary element stress and displacement functions.

2-4 Complete or partial listings of the various programmes.

CHAPTER 2   DEFINITION OF TERMS AND GOVERNING EQUATIONS

The notation used here is the normal Cartesian tensor notation with summation over repeated indices and the comma representation of partial differentiation. The basic equations presented in 2.1 and 2.2 are derived by Cruse (1969), Starfield and Crouch (1973) or Lachat and Watson (1976).

2.1   Boundary element formulation

The region of interest or rock mass may be divided into a number of subregions $R^{(k)}$, each of which may have different elastic constants $E^{(k)}$ and $\nu^{(k)}$. Let $x = (x_1, x_2, x_3)$ be the global co-ordinates of a point in orthogonal Cartesian co-ordinates.

A surface denotes the interface area between two subregions or any surface upon which tractions and/or displacements are specified. The surfaces of each subregion are divided into a number N of triangular or quadrilateral planar elements ΔS_m over which tractions t_i (m) and displacements u_i (m) are constant (i=1,2,3) (m=1,2...N). The system of integral equations which governs the interaction between tractions and displacements is given (Cruse, 1969) by

$$\tfrac{1}{2} u_i^{(k)}(m) + \sum_{n=1}^{N} u_j(n) \int_{\Delta S_n} T_{ij}^{(k)}(m,n)\, dS(n)$$
$$= \sum_{n=1}^{N} t_j(n) \int_{\Delta S_n} U_{ij}(m,n)\, dS(n) \tag{1}$$

for the kth subregion.

The tractions and displacements appear outside the integral signs in (1) because of the assumption of constant tractions and displacements over each element. In (1) element m is termed a receiving element while elements n are termed emitting elements, ie an emitting element n influences the displacements and tractions of a receiving element m via the influence coefficients

$$\int_{\Delta S_n} T_{ij}^{(k)}(m,n)\, dS(n)$$

and

$$\int_{\Delta S_n} U_{ij}^{(k)}(m,n)\, dS(n)$$

(2)

The subscripts i and j relate the relevant components of traction or displacement in the global co-ordinate system. Cruse (1969) evaluates the integrals in (2) analytically. It is possible to evaluate these integrals numerically (except with m = n) with considerable time saving in most cases. The integrals in which m = n are termed "element self effects" and are evaluated as described by Cruse (1969). Numerical evaluation of the integrals in (2) is discussed in more detail in Chapter 3.

Once the surface tractions and displacements are known the stresses $\sigma_{ij}(y)$ and displacements $u_i(y)$ at other points y in the kth subregion are given (1) by

$$u_i^{(k)}(y) = -\sum_{n=1}^{N} u_j^{(k)}(n)\, \Delta T_{ij}^{(k)}(y,n)$$
$$+ \sum_{n=1}^{N} t_j^{(k)}(n)\, \Delta U_{ij}^{(k)}(y,n)$$

(3)

$$\sigma_{ij}^{(k)}(y) = -\sum_{n=1}^{N} u_l^{(k)}(n)\, \Delta S_{lij}(y,n)$$
$$+ \sum_{n=1}^{N} t_l^{(k)}(n)\, \Delta D_{lij}(y,n)$$

(4)

where $\Delta T_{ij}(y,n)$ and $\Delta U_{ij}(y,n)$ are the integrals in (2)

and

$$\Delta S_{lij}^{(k)}(y,n) = \int_{\Delta S_n} S_{lij}^{(k)}(y,n)\, dS(n)$$

$$\Delta D_{lij}^{(k)}(y,n) = \int_{\Delta S_n} D_{lij}^{(k)}(y,n)\, dS(n)$$

(5)

The (k) superscript for the kth subregion is dropped henceforth for convenience where not necessary. The functions T,U,S and D are given (Cruse, 1969) by

$$T_{ij}(m,n) = \frac{c}{4\pi r^2}\left[\frac{\partial r}{\partial n}\left(\delta_{ij} + \frac{3}{1-2\nu}r_{,i}\,r_{,j}\right) - n_j\,r_{,i} + n_i\,r_{,j}\right]$$

$$U_{ij}(m,n) = \frac{1}{4\pi\mu r}\left[\frac{3-4\nu}{4(1-\nu)}\delta_{ij} + \frac{1}{4(1-\nu)}r_{,i}\,r_{,j}\right]$$

$$S_{kij}(m,n) = \frac{c\mu}{2\pi r^3}\left\{3\frac{\partial r}{\partial n}\left[\delta_{ij}\,r_{,k} + \frac{\nu}{1-2\nu}\left(\delta_{ki}\,r_{,j} + \delta_{kj}\,r_{,i}\right)\right.\right.$$
$$\left.- \frac{5}{1-2\nu}r_{,i}\,r_{,j}\,r_{,k}\right] + \frac{3\nu}{1-2\nu}\left(n_i\,r_{,j}\,r_{,k} + n_j\,r_{,i}\,r_{,k}\right)$$

$$\left.+ 3n_k\,r_{,i}\,r_{,j} + n_j\,\delta_{ki} + n_i\,\delta_{kj} - \frac{1-4\nu}{1-2\nu}n_k\,\delta_{ij}\right\} \quad (6)$$

$$D_{kij}(m,n) = \frac{c}{4\pi r^2}\left(\delta_{ki}\,r_{,j} + \delta_{kj}\,r_{,i} - \delta_{ij}\,r_{,k}\right.$$
$$\left.+ \frac{3}{1-2\nu}r_{,i}\,r_{,j}\,r_{,k}\right)$$

where ij is the Kronecker Delta Function

$$r = \left[\left(x_i(n) - x_i(m)\right)\left(x_i(n) - x_i(m)\right)\right]^{1/2} \quad (7)$$

$$r_{,i} = \frac{\partial r}{\partial x_i}$$
$$= \frac{1}{r}\left(x_i(n) - x_i(m)\right) \quad (8)$$

$$\frac{\partial r}{\partial n} = r_{,i}\,n_i \quad (9)$$

$$c = (1-2\nu)\big/ 2(1-\nu)$$

$$n_i = n_i(n) = \text{outward unit normal vector to the emitting element}$$

μ = shear modulus

The equations (1), (3) and (4) form the basis of the first programme BEM of this dissertation. u_i (n) or t_i (n) is specified for each element for i = 1,2,3 except where the element represents an interface to another subregion. The boundary conditions at interface elements (between subregions (k) and (k+1) say) are

$$u_i^{(k)} (n) = u_i^{(k+1)} (m)$$

$$\text{(10)}$$

$$t_i^{(k)} (n) = -t_i^{(k+1)} (m)$$

unless failure of the interface occurs. A mechanism for allowing failure to occur is discussed in Chapter 5. The equations (1), (3), and (4) are further modified to include the "lumping mechanism", various symmetry conditions and the above interface elements.

2.2 Displacement discontinuity formulation

Consider now a plane, relatively thin excavation which is treated here as a single plane surface of negligible thickness. This plane may be divided up into a mesh or grid of square displacement discontinuity elements. A particular element is denoted by its row and column number in the grid (Fig 2.1), ie element ij lies in the ith row and j^{th} column of the grid. Define a local co-ordinate system for this grid (Fig 2.1) so that the x- and y-axes point in the directions of increasing row and column numbers respectively. Let the x-y plane be separated into two surfaces within the mesh the top surface (outward normal points down) being denoted by the + superscript and the bottom surface by a-. A displacement discontinuity arises when these two surfaces move relative to one another. If, as before, it is assumed that displacements and surface tractions are constant over each element then constant displacement discontinuity components may be defined for each element ij by

$$d_\alpha (i,j) = u_\alpha^- (i,j) - u_\alpha^+ (i,j) \quad (\alpha = 1,2,3) \quad \text{(11)}$$

GLOBAL CO-ORDINATE
SYSTEM
Z

Y

X

LOCAL CO-ORDINATE
SYSTEM
Z

ELEMENT (ij).

COL. J

ELEMENT (n).

Y

BOUNDARY ELEMENT
MESH

ROW I.

X

DISPLACEMENT
DISCONTINUITY
GRID
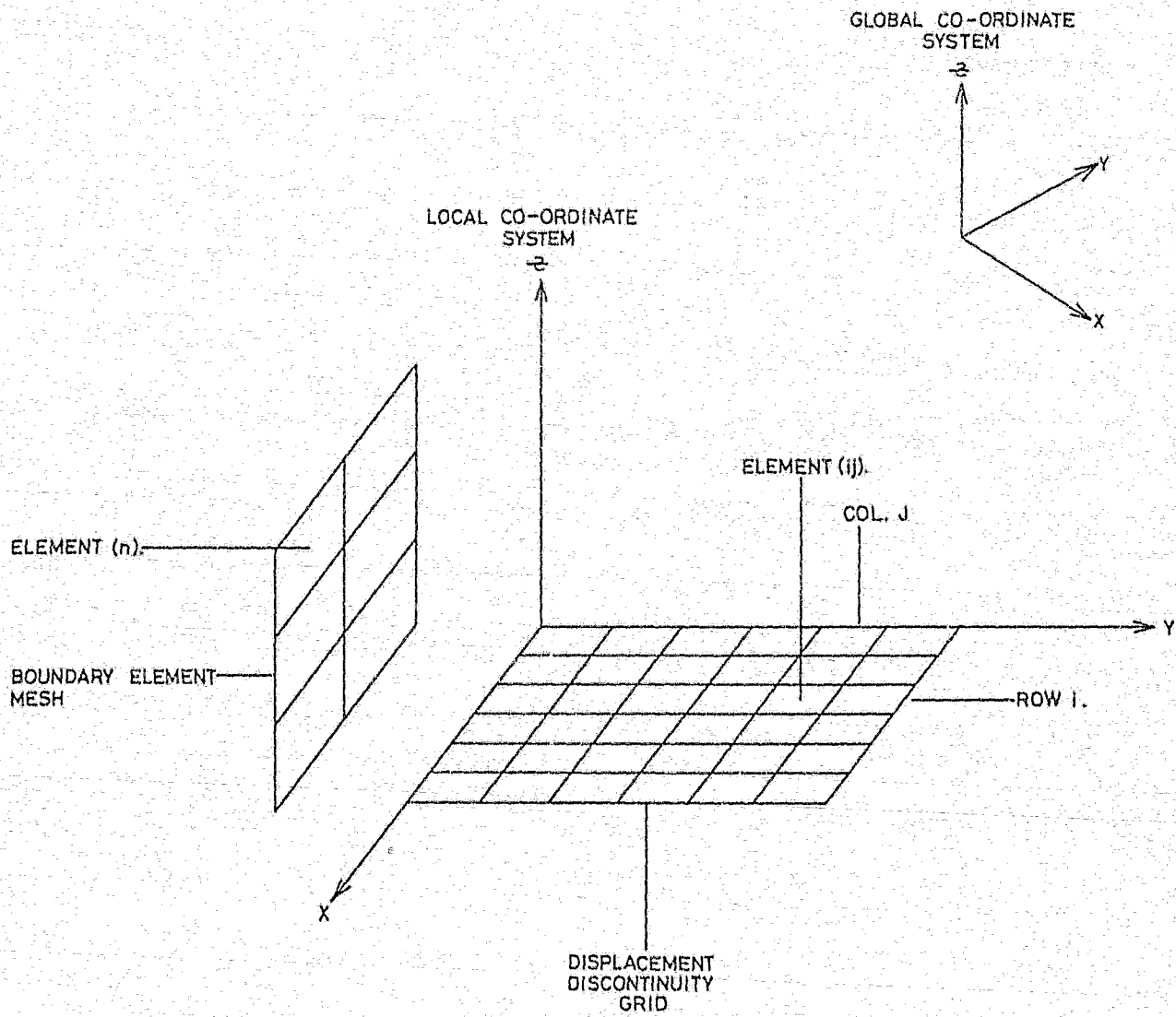
FIG. 2.1   DISPLACEMENT DISCONTINUITY GRID RELATIVE TO THE
BOUNDARY ELEMENT MESH SHOWING LOCAL AND
GLOBAL CO-ORDINATE AXES.

The surface tractions acting on the + and − surfaces of any displacement discontinuity element have equal magnitude but opposite sign. It is more covenient therefore to consider stresses acting "within" an element. The sign conventions adopted are positive normal stresses denoting compression and the normal displacement discontinuity is positive if the + and − surfaces move towards one another (as is normally the case under the action of a compressive stress field).

The normal and shear stresses acting on a displacement discontinuity element i,j are given by

$$\sigma_{13} (i,j)$$
$$\sigma_{23} (i,j)$$
$$\sigma_{33} (i,j)$$

in the local co-ordinate system chosen. Starfield and Crouch (1973) give equations relating these normal and shear stresses to the normal and shear displacement discontinuity components

$$\sigma_{\alpha 3} (i,j) = \sum_{k=1}^{M} \sum_{\ell=1}^{M} K_{\alpha\beta} (i,j,k,\ell) \, d_{\beta} (k,\ell) \tag{12}$$

$$(\alpha, \beta = 1,2,3)$$

where there are M rows and columns in the grid and K denotes an influence coefficient similar to the T coefficients described earlier. These coefficients K may be evaluated in closed form (Starfield and Crouch, 1973) for square displacement discontinuity elements lying in the same plane and may be expressed in terms of row and column differences i-k and j-l.

The stresses and displacements at points y outside the grid are given (see Appendix 1) by

$$u_{\alpha} (y) = - \sum_{k=1}^{M} \sum_{\ell=1}^{M} d_{\beta} (k,\ell) \, \Delta T_{\alpha\beta} (y,k,\ell) \tag{13a}$$

$$\sigma_{\alpha\beta} (y) = \sum_{k=1}^{M} \sum_{\ell=1}^{M} d_{\gamma} (k,\ell) \, \Delta S_{\gamma\alpha\beta} (y,k,\ell) \tag{13b}$$

The form of (13a) and (13b) is very similar to that of (3) and (4). The coefficients T (y,k,l) and U(y,k,l) are evaluated numerically using the functions given in (6). The additional index in these terms is used purely to indicate the row and column of a displacement discontinuity element as opposed to an element number for boundary elements. The surface tractions acting upon a displacement discontinuity element do not affect the stresses and displacements elsewhere in the body so that the U and D terms in (3) and (4) are not present in (13a) and (13b). When evaluating the T and S functions for a displacement discontinuity element, the outward normal of the bottom (-) surface is chosen in keeping with the definition of d(i,j) in (11).

2.3 Equations for mixed boundary element method

In order to derive the equations for the mixed boundary element method, it is necessary first to convert the co-ordinates, tractions, displacements and normal vectors of the boundary elements to the local co-ordinate system of the displacement discontinuity elements. The necessary transformations are

$$
\begin{aligned}
u_\alpha &= \ell_{\alpha i}\, u_i \\
t_\alpha &= \ell_{\alpha i}\, t_i \\
x_\alpha &= \ell_{\alpha i}\,(x_i - x_i') \\
n_\alpha &= \ell_{\alpha i}\, n_i
\end{aligned}
\qquad\text{etc}\quad (14)
$$

where $\ell_{\alpha i}$ are the direction cosines of the local with respect to the global co-ordinate system.

and x'_i is the origin of the local with respect to the global co-ordinate system.

Once these quantities have been evaluated, there is no further need to consider the global co-ordinate system and the i,j and k subscripts of equations (1) to (9) are merely replaced by Greek subscripts α, β, γ etc. (This avoids confusion with the i,j,k and l values for rows and columns).

The equations (1), (3) and (4) are written for a tension positive stress convention while the corresponding equations for the displacement discontinuity elements are written for a compression positive convention. The equations which follow take this into account and are written for the latter convention.

Let an entire displacement discontinuity grid be placed within the first subregion of boundary elements. Stresses and displacements at points y inside this subregion are given by a summation of equations (3) and (4) with (13a) and (13b) –

$$u_\alpha(y) = -\sum_{n=1}^{N}\left[u_\beta(n)\,\Delta T_{\alpha\beta}(y,n) + t_\beta\,\Delta U_{\alpha\beta}(y,n)\right]$$
$$-\sum_{k=1}^{M}\sum_{\ell=1}^{M} d_\beta(k,\ell)\,\Delta_{\alpha\beta}(y,k,\ell) \tag{15}$$

$$\sigma_{\alpha\beta}(y) = \sum_{n=1}^{N}\left[u_\gamma(n)\,\Delta_{\gamma\alpha\beta}(y,n) - t_\alpha(n)\,\Delta D_{\gamma\alpha\beta}(y,n)\right]$$
$$+\sum_{k=1}^{M}\sum_{\ell=1}^{M} d_\gamma(k,\ell)\,\Delta S_{\gamma\alpha\beta}(y,k,\ell) \tag{16}$$

Similarly, the displacements induced at centroids of boundary elements by displacement discontinuity elements must be included in equation (1) and stresses (σ_{13}, σ_{23} and σ_{33} only) induced at displacement discontinuity elements by boundary elements must be included in equation (11) giving

$$\tfrac{1}{2}u_\alpha(m) + \sum_{n=1}^{N} u_\beta(n)\,\Delta T_{\alpha\beta}(m,n) + \sum_{k=1}^{M}\sum_{\ell=1}^{M} d_\beta(k,\ell)\,\Delta T_{\alpha\beta}(m,k,\ell)$$
$$\tag{17}$$
$$= \sum_{n=1}^{N} t_\alpha\,\Delta U_{\alpha\beta}(m,n)$$

for boundary elements and

$$\sigma_{\alpha 3}(i,j) = \sum_{k=1}^{M} \sum_{\ell=1}^{M} K_{\alpha\beta}(i,j,k,\ell) \, d_{\beta}(k,\ell)$$

(18)

$$+ \sum_{n=1}^{N} u_{\gamma}(n) \Delta_{\gamma\alpha\beta}(y,n) - \sum_{n=1}^{N} t_{\alpha}(n) \Delta D_{\gamma\alpha\beta}(y,n)$$

for displacement discontinuity elements

The equations (15) to (18) form the basis of the mixed boundary element programme MBEM. For each element, the stresses or displacements or tractions are specified in (17) and (18) in the x, y and z directions and a linear system of equations results. These equations are then solved iteratively using the method of successive over relaxation (SOR) for the unknown displacements, tractions and displacement discontinuities.

The following points are worth noting about these equations:

(1) They do not include the effects of lumping
(2) Tractions and displacements are both not known a priori at interfaces between subregions but may be found iteratively as described in the fifth chapter.
(3) The numbers of coefficients T, U etc calculated in or used by equations (17) and (18) are

$$9 \times 2 \times N^2 + 9 M^2 N \qquad \text{for} \qquad (17)$$
$$\text{and} \quad 9 \times 2 \times N M^2 + 5 M^4 \qquad \text{for} \qquad (18)$$

Since the coefficients $K(i,j,k,l)$ in (18) depend only upon the differences $i - k$ and $j - l$, and since some of the coefficients may be collected into the vector of known boundary conditions, the number of coefficients which must be stored by the computer in the absence of lumping is at best

$$(9N^2 + 9 \, M^2N) + 9 \, NM^2 + 3 \, M^2 \tag{19}$$

while the number of degrees of freedom in the system is

$$3(N + M^2)$$

For practical problems, $N \geqslant 150$ while $M \geqslant 20$ so that excessive amounts of storage are required. The need for a means of reducing storage requirements is evident.

2.4 Discussion of mixed boundary element method equations

Much attention is currently being given to "hybrid" or mixed stress analysis techniques. Zienkiewicz (1979) gives a comprehensive summary of techniques currently in use for combining finite element and boundary element formulations. Each element type is used to model that part of the problem to which it is best suited. Crouch (1976) has demonstrated how, in two-dimensional problems, the displacement discontinuity method may model both crack or fault type problems as well as open cavity problems. This formulation uses equations similar to (12). It is seen from equation (12) that calculation of "stress" influence coefficients is required as compared with "displacement" influence coefficients (3) required for a boundary element formulation. Use of the latter type of influence coefficient for open cavity type problems is to be preferred for the following reasons:

(i) If influence coefficients are being evaluated using numerical integration (no closed form solution to the integral $K_{\alpha\beta}(i,j,i,j)$ in (12) for an arbitrary quadrilateral or triangle was found in the literature) then the time required to evaluate "displacement" coefficients is significantly less

than that required for the equivalent stress coefficients. In addition, all integrations may be done with respect to a single co-ordinate system whereas the "stress" coefficients have to be transformed to the local co-ordinate system of each element if this does not coincide with the global co-ordinate system.

(ii) Crouch (1976) shows how, when dealing with an open cavity, the displacement discontinuity formulation produces an interior and an exterior region. Some problems arise with the interior region if no restraints are made to prevent rigid body motion. No such problems arise with the boundary elements since there is not more than one region under consideration.

Conversely, numerous problems arise when attempts are made to use boundary elements to model a tabular excavation or a crack type problem.

It is logical therefore, to match element types to the problem. Moreover, since most tabular excavations are nearly planar it is economic to model such an excavation with a regular grid of square displacement discontinuity elements. An open pit or open excavation is likely to have an irregular shape necessitating the use of triangular or quadrilateral elements.

Equations (15) to (18) are derived for the class of problem in which tabular and open excavations are present. This is a class of problems which arises fairly frequently in mining rock mechanics.

CHAPTER 3 NUMERICAL INTEGRATION OF INFLUENCE COEFFICIENTS

The following integrals or influence coefficients have to be evaluated numerically in the boundary element or mixed boundary element formulations:

$$\Delta\, T_{\alpha\beta}\,(y,n)$$
$$\Delta\, U_{\alpha\beta}\,(y,n)$$
$$\Delta\, S_{\gamma\alpha\beta}\,(y,n)$$
$$\Delta\, D_{\gamma\alpha\beta}\,(y,n)$$

The method of integrating these functions over a flat triangle is the same for each function even if the resulting accuracies differ slightly. It is therefore only necessary to describe the evaluation of $T(y,n)$. Three separate cases exist:

(i)   Triangular boundary elements
(ii) Quadrilaterial boundary elements
(iii) Square displacement discontinuity elements

3.1 Boundary elements

The quadrilateral elements are simply divided into two triangular elements which are then treated separately. The function $T(y,n)$ varies over the surface of the nth triangle, (an emitter triangle). The rate of variation depends primarily on the distance separating the emitting triangle n from the receiving point y and the size of the element and to a lesser extent upon the orientation, and shape of the emitting element.

The method of evaluating the integral is equivalent to first estimating an average value of the function over the element and then multiplying this value by the area of the triangle.

If a is the area of the emitting triangle and r the distance to the point y then a measure of the variation of the function T over the triangle is given by the ratio R.

$$R = r^2/a \qquad (20)$$

(See Fig 3.1)

In each case R is evaluated and the number of points at which T is to be evaluated over the triangle in order to give sufficient accuracy is determined. The options are 1, 3, 7, 21 and 42 points. The points at which the function is to be evaluated are given in Table 3.1 for the 1, 3 and 7 point cases Zienkiewicz (1971)

TABLE 3.1 : CO-ORDINATES AND WEIGHTS FOR 1, 3 AND 7 POINT INTEGRATION

No of points	Weight	Triangular co-ordinates ζ_i		
1	1.000	1/3	1/3	1/3
3	0.33333	1/2	1/2	0
	0.33333	0	1/2	1/2
	0.33333	1/2	0	1/2
7	W_1	1/3	1/3	1/3
	W_2	a_1	b_1	b_1
	W_2	b_1	a_1	b_1
	W_2	b_1	b_1	a_1
	W_3	a_2	b_2	b_2
	W_3	b_2	a_2	b_2
	W_3	b_2	b_2	a_2

with

$$a_1 = 0.05961587$$
$$b_1 = 0.47014206$$
$$a_2 = 0.79742699$$
$$b_2 = 0.10128651$$

$$w_1 = 0.225$$
$$w_2 = 0.13239415$$
$$w_3 = 0.12593918$$

A point x say, within triangle n, at which the function T is to be evaluated is given by

$$x_\alpha(k_n) = \zeta_1(k) x_\alpha^1(n) + \zeta_2(k) x_\alpha^2(n) + \zeta_3(k) x_\alpha^3(n)$$

$$= \zeta_\beta(k) x_\alpha^\beta(n) \quad, \qquad \alpha = 1,2,3 \qquad (21)$$

1   POINT INTEGRATION

3   POINT INTEGRATION

7   POINT INTEGRATION

21 POINT INTEGRATION

42 POINT INTEGRATION

RECEIVING POINT.
EMITTING TRIANGLE.
EMITTING POINT.
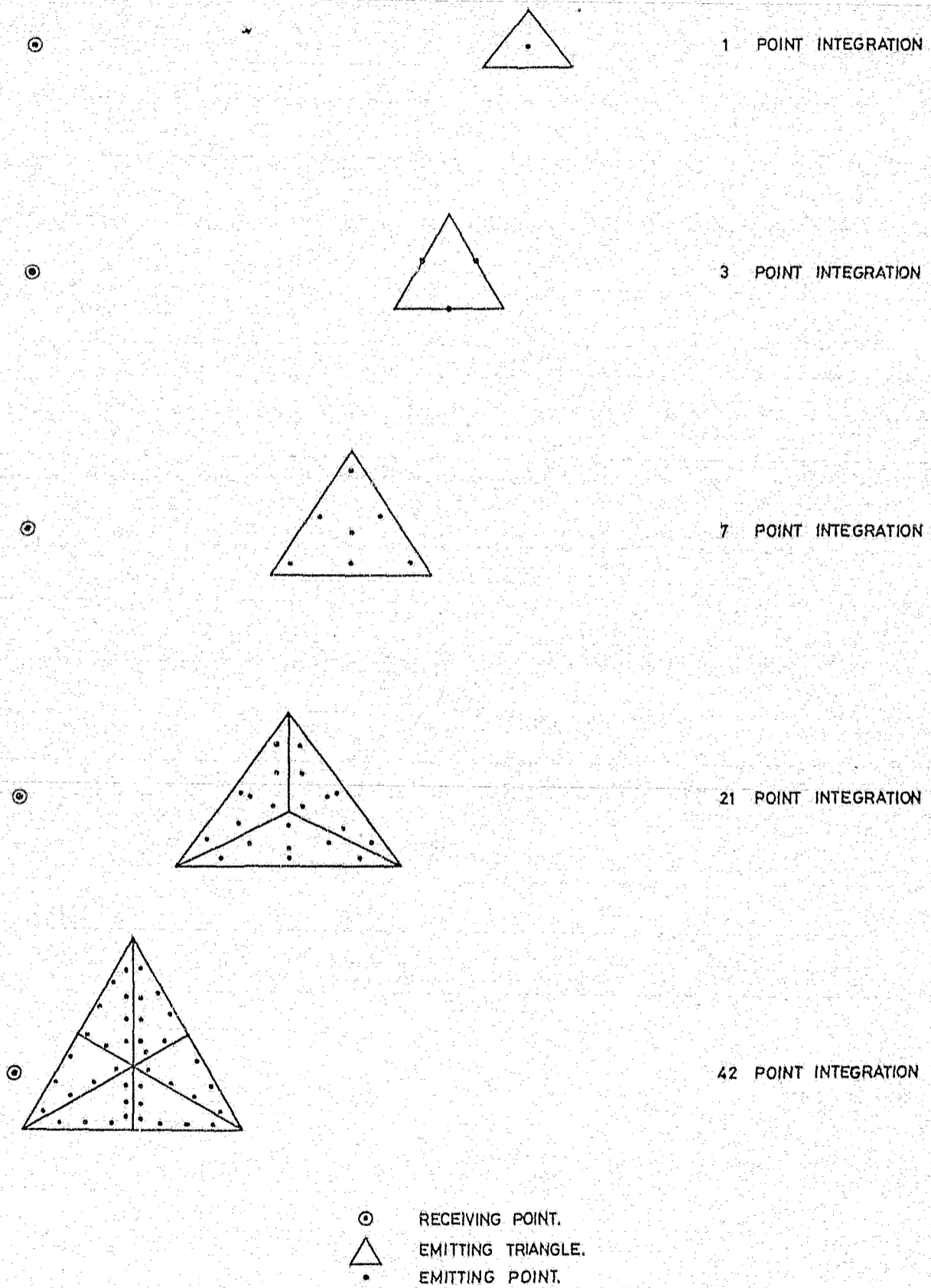
FIG. 3.1   NUMERICAL INTEGRATION SCHEMES FOR TRIANGULAR
BOUNDARY ELEMENTS.

where x_α^β are the co-ordinates of the node β of triangle n and $\xi_\beta(k)$ are the .1). point, (Table 3.1).

Thus

$$\Delta T_{\alpha\beta}(y,n) = a \sum_{k=1}^{I} w_k \, T_{\alpha\beta}\left(y, x(k_m)\right) \tag{22}$$

where I = 1,3 or 7

When 7 point integration is inadequate (ie value of R too small), the triangle is subdivided further into three or six smaller triangles, each of equal area and the 7 point formula is applied in turn to each of these. The nodes of the smaller triangles are merely the nodes or centroids of the original triangle or the midpoints of its sides, (Fig 3.1)

The quadrature algorithm may be summarized as follows:-

(1)   If element n is quadrilaterial, divide into two triangular elements, n and n' say

(2)   Calculate centroid of triangle n $x°(n)$ (or $x°(n')$)

(3)   Calculate $r^2 = (y_i - x_i°(n))(y_i - x_i°(n))$

(4)   Calculate $R = r^2/a$ and decide on the required accuracy 1,3 or 7 point etc (a = triangle area)

(5)   Evaluate the outward normal to triangle n = n(n)

(6)   Subdivide triangle n into 1,3 or 6 subtriangles and calculate additional nodal co-ordinates for the subtriangles (m) if necessary

(7)   There are 1,3 or 7 sample points within each subtriangle (m)

For each sample point k inside subtriangle m:

(a) evaluate its co-ordinate $x_\alpha (k_m)$ from (21)

(b) evaluate r, $r_{,\alpha}$ and $\dfrac{dr}{dn}$ from (7), (8) and (9)

(c) evaluate the functions $T_{\alpha\beta}(y,x(k_m))$, $U_{\alpha\beta}(y,x(k_m))$ etc as required

(d) continue evaluation of $\Delta T_{\alpha\beta}(y,n)$ etc from (22)

Although the different functions T, U, S and D are inversely proportional to r, r^2 or r^3, it is convenient from a programming point of view to evaluate them together as described above.

There are several secondary benefits arising from this point integration scheme. A continuous check on the ratio R at each integrand point enables errors in the data input to be easily detected.

Fig 3.2 shows a common example in which a node of an element is incorrectly specified. Such errors are easily overlooked when checking the data manually since the area, outward normal and position of the element may all be correct. If the ratio R drops below some threshold value R_{min}, say, during the integration procedure, the error is easily detected. If elements are so close that a 42 point integration formula is unreliable, then it is highly probable that a bad choice of element sizes has been made and that the iterative solution would converge very slowly or not at all.

When lumping is implemented, it is possible, by using only 1 point integration, to quickly assess the amount of storage which will be required. If the maximum available storage is exceeded, then a coarser lumping mechanism may be adopted without wasting too much time.

GAP

ELEMENT (n) ———————————— ELEMENT (m).

R
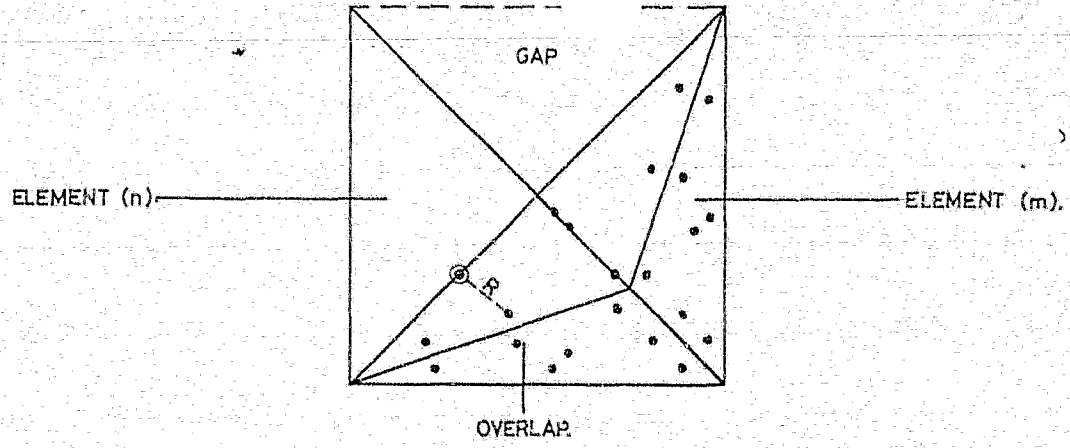
OVERLAP.

a). ELEMENT (m) HAS ONE NODE INCORRECTLY SPECIFIED CAUSING ELEMENT OVERLAP. A VERY SMALL DISTANCE 'R' RESULTS.

ELEMENT (m).

R
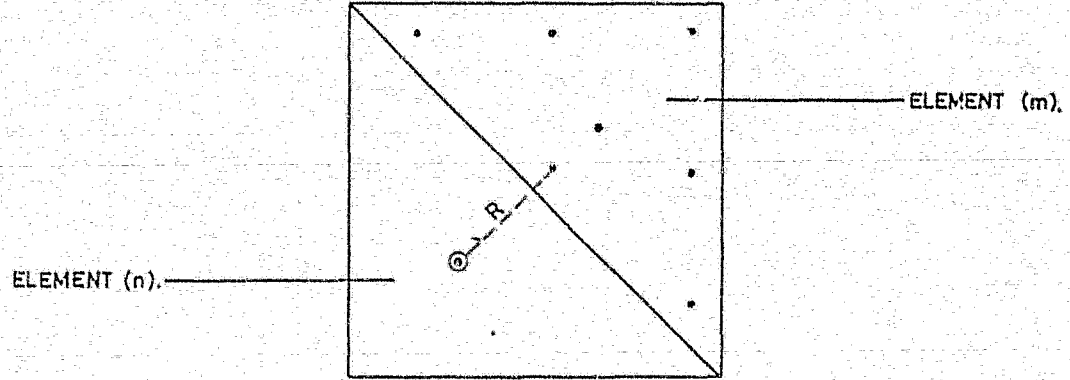
ELEMENT (n).

b). ELEMENTS (n) AND (m) ARE CORRECTLY SPECIFIED AND DISTANCE 'R' IS NOT TOO SMALL.

⊙ RECEIVING POINT.

△ EMITTING TRIANGLE.

• EMITTING POINT.

FIG. 3.2   DETECTION OF INPUT DATA ERRORS DURING NUMERICAL INTEGRATION.

3.2 Displacement discontinuity elements

The displacement discontinuity elements are all square so that implementation of a Gauss Quadrature formula is simple, accurate and efficient. For each element the ratio R is evaluated as before and 1, 4, 9 or 64 point formulae are selected accordingly. (22) is rewritten for displacement discontinuity element ij as -

$$\Delta T_{\alpha\beta}\left(y,i,j\right) = a \sum_{k=1}^{I} w_k\, T_{\alpha\beta}\left(y, x\left(k,i,j\right)\right) \qquad (23)$$

The use of square elements enables the integrand points $x(k,i,j)$ to be evaluated efficiently in terms of the element centoid and element half width. The Gauss Quadrature coefficients were taken from Zienkiewicz (1971). Also since it is known that the outward normal to all displacement discontinuity elements is $(0,0,1)$, considerable simplifications may be made to the functions T and S.

3.3 Discussion

Briefly, the advantanges of the numerical integration may be summarized as follows:

(i) A comprehensive check on the input data is made avaiable

(ii) For most problems, the numerical integration is quicker than analytic integration. For some geometries, this might not be true, however

(iii) It is not necessary to evaluate or invert the Jacobian matrix at every integration point

(iv) A trade off between accuracy and execution time is available. This was found to be very useful in the development stage of the programmes.

It should also be noted that the element self effects (for which $r=0$) are evaluated analytically due to the presence of the $1/r$ singularities. The displacement discontinuity coefficients K (18) are also evaluated analytically facilitating the use of a recurrence formula described by Starfield and Crouch (1973).

CHAPTER 4   DESCRIPTION OF LUMPING MECHANISM

The lumping mechanism described here is essentially an extension of the numerical quadrature procedure described in Chapter 3.   When emitting, elements are remote from receiving elements, then the functions

$$T_{\alpha\beta}(y,n)$$
$$U_{\alpha\beta}(y,n)$$
$$S_{\gamma\alpha\beta}(y,n)$$
$$D_{\gamma\alpha\beta}(y,n)$$

vary slowly over the emitting elements.   When this occurs, the coeffi- cients for a number of elements may be grouped into a single lump coeffi- cient.   The lumping mechanism has already been put to great use in existing boundary and displacement discontinuity formulations (Starfield and Crouch (1973) and Deist and Georgiadis (1976)) but these schemes differ somewhat from the scheme outlined below.

4.1   Boundary element lumping

When a mesh of boundary elements is being drawn up, the user is required to group elements with similar orientation, size and location into "lump elements" containing from one to twelve boundary elements.   (The extra effort required to do this is more than off-set by the additional error checks which become available).   Consider two lump elements with 4 boundary elements in each (Fig 4.1).   Let the "receiver" lump contain 4 potential receiving elements and the "emitter" lump 4 potential emitter elements.   In the absence of any lumping mechanism, 4x4 = 16 sets of coefficients have to be calcu- lated (there are 18 coefficients in each set).   If the 4 emitting elements are grouped together then each receiving element requires a different set of coefficients, ie. 4 sets are required.   If the receiving elements are grouped together then only 1 coefficient set is required.

The three types of coefficient set are referred to as element-element, lump-element and lump-lump coefficients respectively
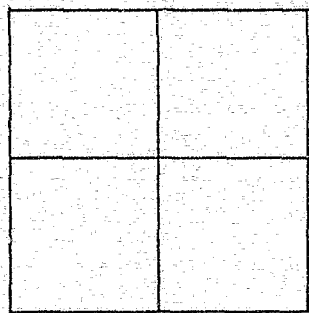
RECEIVER LUMP
(4 ELEMENTS)
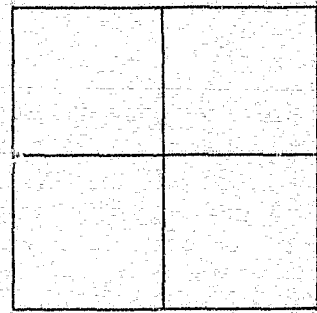
EMITTER LUMP
(4 ELEMENTS)
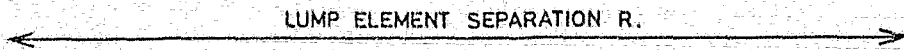
LUMP ELEMENT SEPARATION R.

FIG. 4.1   FORMATION OF LUMP ELEMENTS FOR NUMERICAL INTEGRATION

(See Fig 4.2). If lumps are chosen to be nearly planar or planar
then the centroids, areas and outward normals of the lump elements
may be calculated just as for normal elements.

In deciding which coefficient type to use, the ratio

$$R = \frac{r^2}{a} \quad \text{is used}$$

as before where r = distance separating the lump centroids
              a = area of emitting lump

The potential time and storage savings of this lumping scheme improve
as the number of elements increase. If boundary elements alone are
considered, then the number of coefficients required for an N element
problem in the absence of lumping is

$$18 \, N^2$$

If the average number of elements per lump is 6, say, then the number
of lumps is

$$M \approx N/6$$

and if approximately 40 element-element coefficients are required per
element, then the approximate number of coefficients required with
lumping is

$$18 \, N\left[\frac{N}{6} + 40 + \frac{N}{36}\right]$$

The storage and time-saving factor for N = 300 is therefore about 3.
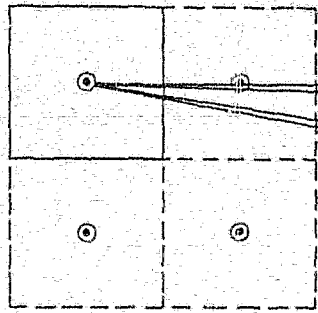
4 RECEIVING ELEMENTS
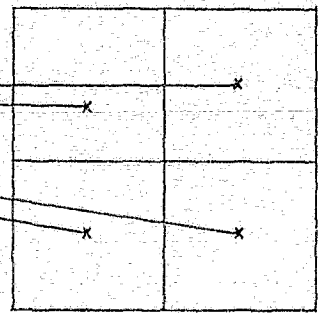
4 EMITTING ELEMENTS

16 ELEMENT–ELEMENT CO–EFFICIENTS
(ONLY 4 SHOWN FOR CLARITY)
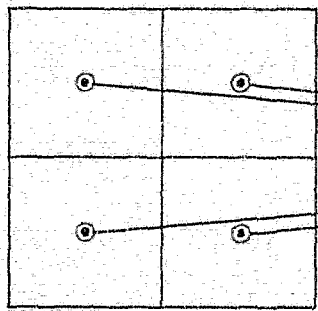
4 RECEIVING ELEMENTS
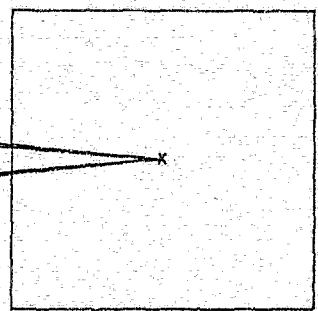
1 EMITTING LUMP

4 LUMP–ELEMENT CO–EFFICIENTS
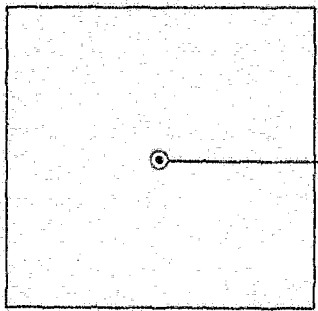
1 RECEIVING LUMP
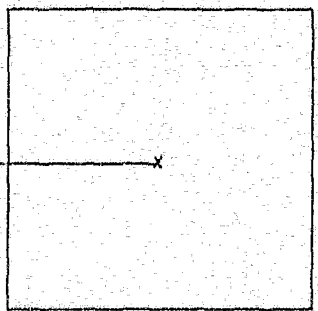
1 EMITTING LUMP

1 LUMP–LUMP CO–EFFICIENT

FIG. 4.2   DIFFERENT TYPES OF INFLUENCE CO–EFFICIENTS.

The lump elements are treated just as ordinary elements, and lump displacements, tractions, normals and areas are calculated as averages weighted with element areas. The lumping mechanism is directly applicable to the evaluation of interior stresses and displacements. At present all lump coefficients are evaluated by one point integral formulae, but it is expected that greater savings would be obtained by using higher order formulae for these coefficients, since emitting lump elements could effectively be brought closer to receiving elements, thus further reducing the total number of coefficients.

4.2 Displacement discontinuity lumping

Two separate schemes are adopted for evaluation of element-element interactions and for evaluation of stresses and displacements at interior points. The former scheme is based on that of Starfield and Crouch (1973) while the latter is essentially that described above.

For evaluation of element-element coefficients, groups of 1,4, 9 or 25 displacement discontinuity elements are grouped into square lump elements and lump-lump or element-element coefficients only are calculated. The need for the lump-element coefficients described above is obviated apparently because the relevant integrals are evaluated in closed form, not numerically.

4.3 Reduction of storage requirements

While the lumping scheme described above was initially implemented to reduce disk storage requirements and execution time, a number of other benefits also result, the most important being a reduction in core storage requirements.

In the absence of lumping, it is expedient to hold in main memory the following arrays.

nodal co-ordinates
element areas

element displacements
element tractions
element direction cosines
element centroids
element-node numbering
element codes

Once lumping is introduced it becomes necessary to keep track of the integration scheme (lump-lump, lump-element or element-element) used for each lump element. If there are M lumps, then this array is of dimension MxM.

Once interface elements are introduced, it is necesary also to store for each lump element information such as cohesion and angle of friction (Chapter 5) as well as the direction cosines of a local co-ordinate system for each element.

Before implementation of the storage reduction scheme, it was found that core storage limited the maximum number of elements to about 500. With 500 elements however, execution time was increased since it was easier to calculate element centroids and direction cosines as required rather than store them permanently.

Since elements are always accessed through their parent lump element, it is possible to retain in main memory element properties only for those lumps under consideration. For example, a receiver lump and an emitting lump element are retained in main memory during calculation of influence coefficients. To reduce the number of disk transfers required to implement this scheme, all of the lump element arrays (lump areas, displacements etc) are stored in main memory. Main memory requirements are then restricted by the number of lump elements, rather than ordinary elements.

The element properties for any lump element are stored on disk using labelled common arrays (standard for Ascii Fortran IV). This enables the use of a direct disk access routine reducing further the disk access times.

4.4 Lumping - a brief discussion

The lumping system described here is designed specifically for the
boundary integral type of equation. It is ideal for systems
requiring disk or tape storage because of the sequential access of
data. It is also ideal for systems of equations which are diagonally
dominant and hence well suited to iterative solution techniques. The
lump variables (displacements and tractions) are calculated as
weighted averages of their constituent elements. As such it is
possible to implement this lumping mechanism into systems of equa-
tions which are being solved using an elimination rather than an
iterative technique. The total number of degrees of freedom of the
system would be increased by about 10 percent. This new system of
equations would also be about 15 to 50 percent populated but unfort-
unately would not be a banded system. Special elimination techniques
which minimize the amount of "fill in" (zero coefficients which
become non-zero in the elimination process) would be required. In
addition, the simple sequential access of coefficients used in the
iterative solution is not applicable to elimination schemes. Disk or
coefficient access tends to be more random. Finally, elimination
schemes are not well suited to the modelling of non-linear behaviour
which occurs when failure of material interfaces is initiated.

Gaussian elimination may be compared with successive over relaxation
(SOR) for a problem of 1 000 elements or 3 000 degrees of freedom as
follows:

<center>Gaussian Elimination (SOR)</center>

	Gaussian Elimination	(SOR)
Number of coefficients	9×10^6	2×10^6
Number of arithmetic	$1/3 \ N^3$	$2 \times 10^6 \times 2$ per iteration
adds and multiplies	ie 9×10^9	ie $\pm 6 \times 10^7$

For such a problem, the iterative solution is up to 150 times more
efficient than elimination without the lumping mechanisms.

The lumping scheme, as implemented in this dissertation is applied to the simplest boundary element type, namely the constant displacement/traction element. Although not an express aim of this dissertation, it is felt that lump elements provides a reasonable alternative to the more sophisticated element types (quadratic and cubic variation of unknowns over each element) of Lachat and Watson (1976).

Alternatively, a marked improvement in the performance of these higher order elements could be expected if they could be lumped.

CHAPTER 5   DESCRIPTION OF BOUNDARY INTERFACE ELEMENTS AND SYMMETRY
            CONDITIONS

Consider the simple problem shown in Figure 5.1 of two subregions each
containing 2 elements (after Lachat and Watson (1976)). Each element is a
schematic representation of a number of simple planar elements which would
constitute each subregion. The boundary conditions are such that trac-
tions are specified at elements 1 and 4 while stresses and displacements
are continuous across the interface between the two subregions. Assume
further, for the moment, that the problem only has displacements and trac-
tions in one dimension. Equation (1) may be written in matrix form for
the problem as -

$$\begin{bmatrix} T(1,1) & T(1,2) & 0 & 0 \\ T(2,1) & T(2,2) & 0 & 0 \\ 0 & 0 & T(3,3) & T(3,4) \\ 0 & 0 & T(4,3) & T(4,4) \end{bmatrix} \begin{bmatrix} u(1) \\ u(2) \\ u(3) \\ u(4) \end{bmatrix} = \begin{bmatrix} U(1,1) & U(1,2) & 0 & 0 \\ U(2,1) & U(2,2) & 0 & 0 \\ 0 & 0 & U(3,3) & U(3,4) \\ 0 & 0 & U(4,3) & U(4,4) \end{bmatrix} \begin{bmatrix} t(1) \\ t(2) \\ t(3) \\ t(4) \end{bmatrix}$$

or by using subscripts for the matrix coefficients:

$$\begin{bmatrix} T_{11} & T_{12} & 0 & 0 \\ T_{21} & T_{22} & 0 & 0 \\ 0 & 0 & T_{33} & T_{34} \\ 0 & 0 & T_{43} & T_{44} \end{bmatrix} \begin{bmatrix} u_1 \\ u_2 \\ u_3 \\ u_4 \end{bmatrix} = \begin{bmatrix} U_{11} & U_{12} & 0 & 0 \\ U_{21} & U_{22} & 0 & 0 \\ 0 & 0 & U_{33} & U_{34} \\ 0 & 0 & U_{43} & U_{44} \end{bmatrix} \begin{bmatrix} t_1 \\ t_2 \\ t_3 \\ t_4 \end{bmatrix}$$

The zero coefficients arise because there is no direct interaction between
the two subregions other than the displacement and traction boundary
conditions at the interface. For this problem these may be written as:-

$$u_2 = u_3$$
$$t_2 = -t_3$$

(25)

ELEMENT 1   ELEMENT 4

SUBREGION 1   SUBREGION 2

ELEMENT 2   ELEMENT 3
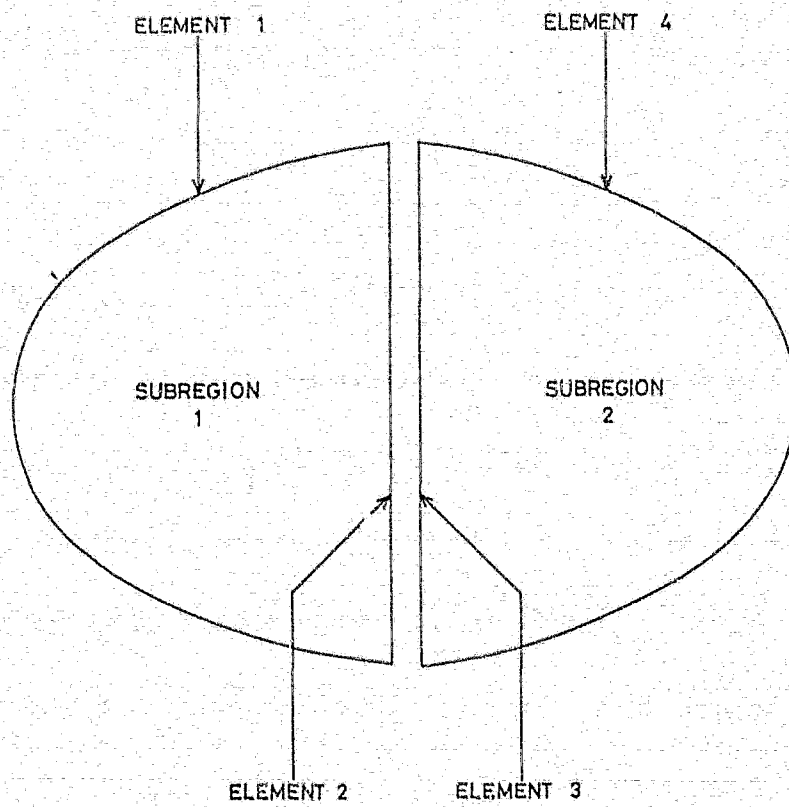
FIG. 5.1   HYPOTHETICAL PROBLEM SHOWING INTERFACE BETWEEN TWO SUBREGIONS.

By sorting known and unknown quantities to the left and righthand sides respectively and applying (25) to (24), (24) may be rewritten as –

$$
\begin{bmatrix}
T_{11}^{(1)} & T_{12}^{(1)} & U_{12}^{(1)} & 0 \\
T_{21}^{(1)} & T_{22}^{(1)} & U_{22}^{(1)} & 0 \\
0 & T_{33}^{(2)} & -U_{33}^{(2)} & T_{34}^{(2)} \\
0 & T_{43}^{(2)} & -U_{43}^{(2)} & T_{44}^{(2)}
\end{bmatrix}
\begin{bmatrix}
u_1^{(1)} \\
u_2^{(1)} \\
t_3^{(2)} \\
u_4^{(2)}
\end{bmatrix}
=
\begin{bmatrix}
U_{11}^{(1)} & t_1^{(1)} \\
U_{21}^{(1)} & t_2^{(1)} \\
U_{34}^{(2)} & t_4^{(2)} \\
U_{44}^{(2)} & t_4^{(2)}
\end{bmatrix}
=
\begin{bmatrix}
b_1 \\
b_2 \\
b_3 \\
b_4
\end{bmatrix}
$$

where superscripts denote the subregion

It has been stated above that the equations (1) or (26) are solved using an iterative scheme (Successive over relaxation). A sufficient, but not necessary, condition for convergence of this scheme is that the system matrix is diagonally dominant (Froberg 1970). Experience has shown that it is only necessary to maintain an approximate degree of diagonal dominance in the system matrix. (The rate of convergence gradually decreases as diagonal dominance decreases). Now the magnitudes of the element self effects T_{ii} and U_{ii} are approximately

$$
T_{ii}^{(k)} \approx \frac{1}{2}
$$

$$
U_{ii}^{(k)} \approx \frac{1}{G(k)}
$$

(27)

where $G(k)$ is the shear modulus for the kth subregion. Also, within any subregion for a well posed problem

$$T_{ii}^{(k)} \gg T_{ij}^{(k)} \quad i \neq j$$

$$U_{ii}^{(k)} \gg U_{ij}^{(k)} \quad i \neq j$$

Let the coefficients $T_{ij}^{(k)}$ and $U_{ij}^{(k)}$ $i \neq j$ be denoted by δ and substitute (27) into (26). Then

$$\begin{bmatrix} \frac{1}{2} & \delta & \delta & 0 \\ \delta & \frac{1}{2} & \frac{1}{G(1)} & 0 \\ 0 & \frac{1}{2} & \frac{-1}{G(2)} & \delta \\ 0 & \delta & -\delta & \frac{1}{G(2)} \end{bmatrix} \begin{bmatrix} u_1^{(1)} \\ u_2^{(1)} \\ t_3^{(2)} \\ u_4^{(2)} \end{bmatrix} = \begin{bmatrix} b_1 \\ b_2 \\ b_3 \\ b_4 \end{bmatrix} \qquad (28)$$

In (28) approximate diagonal dominance may be obtained by scaling the shear moduli $G^{(1)}$ or $G^{(2)}$ if they are approximately equal.

Assume firstly that

$$G^{(2)} = 100 \, G^{(1)}$$
$$G^{(1)} = 2$$

The system matrix in (28) becomes

$$
\begin{bmatrix}
\frac{1}{2} & \delta & \delta & 0 \\[2mm]
\delta & \frac{1}{2} & \frac{1}{2} & 0 \\[2mm]
0 & \frac{1}{2} & \frac{-1}{200} & \delta \\[2mm]
0 & \delta & -\delta & \frac{1}{200}
\end{bmatrix}
\tag{29}
$$

It is seen that the third row is definitely not diagonally dominant while the second row is almost diagnoally dominant. Improved diagonal dominance may be obtained in (29) however by swapping the second and third rows or by a choice of shear moduli so that

$$
G^{(2)} \ll G^{(1)}
$$

Since the programming of row swapping is inconvenient and since it is not generally possible to choose suitable shear moduli the following iterative procedure has been adopted for subregions with very different elastic properties.

(1) For the softer subregion, estimate tractions at the interface.
(2) Use these tractions as specified boundary conditions for the stiffer subregion.
(3) For the stiffer subregion, estimate displacements at the interface.
(4) Use these displacements as specified boundary conditions for the softer subregion.

This iterative cycle is easily included in the overall iterative solution.

Intuitively, large displacements in a soft material produce small stresses while large stresses in a stiff material produce small displacements. The diagonal dominance is therefore interpreted as a large cause producing a small effect rather than vice versa.

A somewhat unfortunate consequence of this limitation of allowable boundary conditions is that it is not possible to model a stiff subregion completely enclosed by softer subregions because there is then no restriction of rigid body displacement in the stiff subregion.

5.1 Failure at an interface

It is possible at any stage during the iterative solution (for the tractions and displacements) to calculate the normal and shear displacements and tractions at any element. Lachat and Watson (1976) show how the equations (1) can be rewritten to give tractions and displacements in a local co-ordinate system for each element. This represents a large amount of additional calculation and an alternative approach is to transform tractions and displacements to some local co-ordinate system only when required. Consider the problem of Fig 5.1 again. Let a local co-ordinate system for any element be defined so that the z-axis is the outward normal and y-axis is horizontal. Let the direction cosines of this "elemental" local co-ordinate system with respect to the co-ordinate system of the displacement discontinuity grid be $\ell_{\alpha\beta}$ and the local displacements and tractions be t'_{α} and u'_{α} respectively. (t'_3 and u'_3 are then normal tractions and displacements).

Then

$$t'_{\alpha} = \ell_{\alpha\beta} \, t_{\beta}$$
$$u'_{\alpha} = \ell_{\alpha\beta} \, u_{\beta}$$

(30)

and

$$t_{\beta} = \ell_{\alpha\beta} \, t'_{\alpha}$$
$$u_{\beta} = \ell_{\alpha\beta} \, u'_{\alpha}$$

The boundary conditions for interface elements are:

tractions specified for stiffer elements
displacements specified for softer elements

A Mohr Coulomb failure criterion is implemented in the iterative solution as follows. Let the cohesion and angle of friction of the interface be c and ϕ respectively. Then the shear strength σ_s of the interface is given by

$$\sigma_s = c + \sigma_n \tan \phi \tag{31}$$

where $\quad \sigma_n = -t_3' + p_3 = $ Total normal stress

$\quad\quad\quad p_3 = $ primitive normal stress

The maximum total shear stress component is given by

$$\tau_{max} = \sqrt{(-t_1' + p_1)^2 + (-t_2' + p_2)^2} \tag{32}$$

If $\tau_{max} \geqslant \sigma_s$ then failure occurs. If σ_n is tensile when failure does occur then the mode of failure is also tensile. If not, then the failure mode is in shear.

5.1.1 Shear failure

Shear failure is implemented simply as a change of boundary conditions for the interface elements. Continuity of normal displacements and stresses must be maintained, but the shear displacements are unknown for both interface elements.

The shear tractions are given by

$$t_1'_{new} = t_1'_{old} \times \frac{\sigma_s}{\tau_{max}} + p_1 \tag{33}$$

$$t_2'_{new} = t_2'_{old} \times \frac{\sigma_s}{\tau_{max}} + p_2 \tag{34}$$

5.1.2 Tensile failure

If tensile failure occurs at an interface, then the newly created void becomes indistinguishable from an open excavation. Tractions (equal but opposite in sign) must then be specified at each interface element so that the total resultant tractions (primitive and induced) at these elements are zero, ie set $t_i' = -p_i$.

These updated tractions and displacements are then transformed back to the global co-ordinate system and the process continued. Other boundary conditions may also be implemented at interfaces. These have been described in detail by Crouch (1976) and Starfield and Crouch (1973). Essentially an interface may or may not have a filling or the interface may be treated as part of a tabular excavation. If the interface has no filling it may still fail in shear or tension. If the interface has a filling then the relative displacement of the interface surfaces is controlled by the stiffness of the fill unless failure occurs. If the interface is mined or open then convergence or separation of the surfaces occurs but a limit to the maximum amount of convergence may be specified. Interface elements are therefore assigned different codes to distinguish their different properties.

Code   7   Interface element with no infill
Code   9   Mined or open with a limit on maximum convergence
Code 10   Tensile failed element
Code 11   Shear failed element
Code 12   Interface element with infill
Code   1   Open element with no limit on maximum convergence

These elements are distinguished from other elements which do not belong to interfaces by their codes. Codes for the other elements are:

Code 1 Open or mined element (tractions specified)

Code 2 Zero displacement or fixed element

Code 3 Element fixed in x direction

Code 4 Element fixed in y direction

Code 5 Element fixed in a z direction

Code 6 Any other specified mixture of boundary conditions

Code 8 Represents the earth's surface (z-co-ordinate = 0)

5.2 Symmetry conditions

Symmetry conditions are easily incorporated into the boundary element programme but have not as yet been incorporated into the displacement discontinuity elements of the mixed boundary element programme. Fig 5.2 shows a two-dimensional example containing 4 subregions in which there are two planes of symmetry, XSYM and YSYM. Subregion 3 is entirely contained within subregion 1. It is therefore not directly affected by its symmetry images in the other three quadrants and therefore does not have any symmetry in itself. It is necessary, therefore, to assign separate symmetry conditions to each subregion. The following codes and symmetry types are catered for:

1 : No symmetry

2 : x symmetry

3 : y symmetry

4 : z symmetry

5 : xy symmetry

6 : xz symmetry

7 : yz symmetry

8 : xyz symmetry

In the example in Fig 5.2 the following symmetry codes would apply:

Subregion 1 : Symmetry Code 5

Subregion 2 : Symmetry Code 2

Subregion 3 : Symmetry Code 1

Subregion 4 : Symmetry Code 5
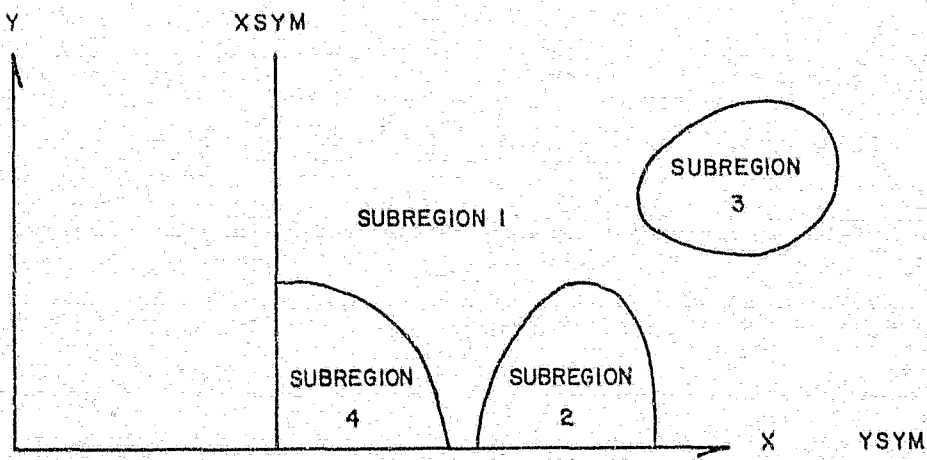
FIG. 5.2   DIFFERENT SYMMETRY CODES FOR A SINGLE PROBLEM

Fig 5.3 shows an example with x and y symmetry. Each of the three images has to be treated separately since for the x image, only x-components of traction, displacement, position etc change while only y-components are affected in the y-image and so on. This is done in the programme by means of two arrays. The first 8x8 array relates different symmetry images to the symmetry code while the second array relates a particular image (x,y or xy etc) to the components of traction, displacement etc that depend upon that image (Table 5.2). In Tables 5.1 and 5.2, 1 denotes "yes" and 0 denotes "no".

TABLE 5.1: SYMMETRY IMAGE – SYMMETRY CODE TABLE (1=Yes, 0=No)

Symmetry Image	Symmetry Code							
	1	2	3	4	5	6	7	8
Object	1	1	1	1	1	1	1	1
x	0	1	0	0	1	1	0	1
y	0	0	1	0	1	0	1	1
z	0	0	0	1	0	1	1	1
xy	0	0	0	0	1	0	0	1
xz	0	0	0	0	0	1	0	1
yz	0	0	0	0	0	0	1	1
xyz	0	0	0	0	0	0	0	1

TABLE 5.2: SYMMETRY IMAGE – x,y,z COMPONENT TABLE (1=Yes, 0=No)

Symmetry Image	Components affected by Image		
	x	y	z
Object	0	0	0
x	1	0	0
y	0	1	0
z	0	0	1
xy	1	1	0
xz	1	0	1
yz	0	1	1
xyz	1	1	1

No detailed description of symmetry was found in the literature but it is expected that this algorithm for the implementation of symmetry is possibly novel (ie different codes for different subregions).
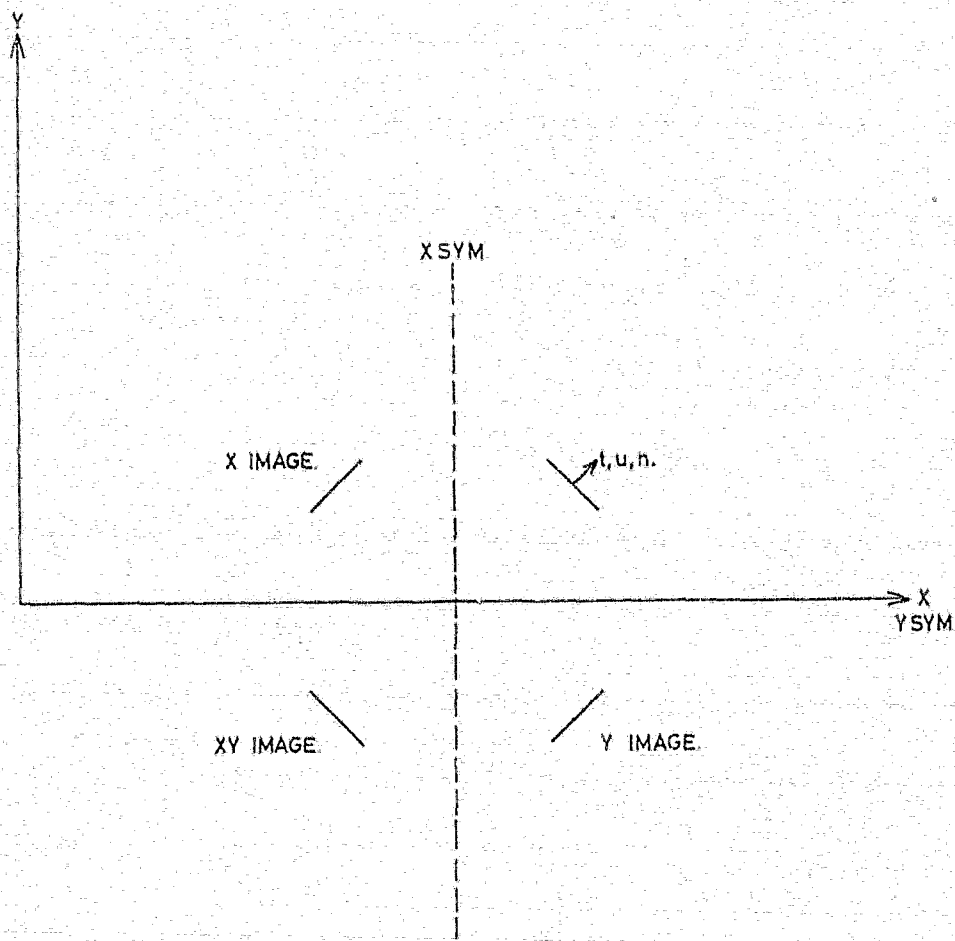
YSYM = PLANE OF Y-SYMMETRY = 0
XSYM = PLANE OF X-SYMMETRY > 0
t = TRACTION
u = DISPLACEMENT
n = ELEMENT NORMAL

FIG. 5.3   IMPLEMENTATION OF SYMMETRY CONDITIONS.

CHAPTER 6   MODIFICATION OF PROGRAMME MINAP FOR NON-HOMOGENEOUS PROBLEMS

The application of the displacement discontinuity method to mining problems in two dimensions has been well demonstrated by Crouch (1976) with his programme MINAP. A restriction of this programme is that it cannot model mining problems in non-homogeneous ground. The programme allows for specification of mixed boundary conditions which makes the incorporation of non-homogeneous subregions into the programme relatively easy.

The basic equations for the two-dimensional displacement discontinuity method have been given, Crouch (1976), for a problem containing N elements (no tensor rotation for summation here).

$$\sigma_s^i = \sum_{j=i}^{N} (A_{ss}^{ij} d_s^j + A_{sn}^{ij} d_n^j)$$

$$\sigma_n^i = \sum_{j=i}^{N} (A_{ns}^{ij} d_s^j + A_{nn}^{ij} d_n^j)$$

(35)

where stresses are specified as boundary conditions

and   j represents an emitting element

     i represents a receiving element

     s represents a shear effect

     n represents a normal effect

       are induced stresses

     d are displacement discontinuities

     A are stress influence coefficients derived by Crouch (1976)

where displacements are specified as boundary conditions,

$$u_s^i = \sum_{j=i}^{N} (B_{ss}^{ij} d_s^j + B_{sn}^{ij} d_n^j)$$

$$u_n^i = \sum_{j=i}^{N} (B_{ns}^{ij} d_s^j + B_{nn}^{ij} d_n^j)$$

(36)

where B are displacement influence coefficients

     u are displacements on one or other of the two displacement discontinuity surfaces.

For example, B^{ij}_{sn} gives the shear displacement induced at element i by the normal displacement discontinuity component of element j.

Consider now the hypothetical problem of Fig 5.1 discussed also in Chapter 5. Stresses are specified at elements 1 and 4, but neither stresses nor displacements are known at elements 2 and 3. Equations (35) and (36) may be written for this problem as

$$
\begin{bmatrix}
A^{11} & A^{12} & 0 & 0 \\
A^{21} & A^{22} & 0 & 0 \\
B^{21} & B^{22} & 0 & 0 \\
0 & 0 & A^{33} & A^{34} \\
0 & 0 & B^{33} & B^{34} \\
0 & 0 & A^{43} & A^{44}
\end{bmatrix}
\begin{bmatrix}
d^1 \\ d^2 \\ d^3 \\ d^4
\end{bmatrix}
=
\begin{bmatrix}
\sigma^1 \\ \sigma^2 \\ u^2 \\ \sigma^3 \\ u^3 \\ \sigma^4
\end{bmatrix}
\tag{37}
$$

where A, B are submatrics given by

$$
A^{ij} = \begin{vmatrix}
A^{ij}_{ss} & A^{ij}_{sn} \\
A^{ij}_{ns} & A^{ij}_{nn}
\end{vmatrix}
$$

$$
B^{ij} = \begin{vmatrix}
B^{ij}_{ss} & B^{ij}_{sn} \\
B^{ij}_{ns} & B^{ij}_{nn}
\end{vmatrix}
$$

and d and σ^i are given by

$$d^i = \begin{bmatrix} d_s^i & d_n^i \end{bmatrix}^T$$

$$\sigma^i = \begin{bmatrix} \sigma_s^i & \sigma_n^i \end{bmatrix}^T$$

Applying the boundary conditions for an interface (10) to (37) gives

$$
\begin{bmatrix}
A^{11} & A^{12} & O & O \\
A^{21} & A^{22} & -A^{33} & -A^{34} \\
-B^{21} & -B^{22} & B^{33} & B^{34} \\
O & O & A^{43} & A^{44}
\end{bmatrix}
\begin{bmatrix}
d^1 \\
d^2 \\
d^3 \\
d^4
\end{bmatrix}
=
\begin{bmatrix}
\sigma^1 \\
O \\
O \\
\sigma^4
\end{bmatrix}
\tag{38}
$$

(38) has the same form as (26) with T replaced by B and U replaced by A.

The equations (38) are not diagonally dominant in general and so the solution of (38) using an interative scheme is also not always possible. These equations may also not be solved by any elimination schemes because of the non-linearities introduced by the fault elements or total closure restrictions essential for most mining applications. As the magnitudes of the B^{22} and B^{33} terms are always equal (they only depend upon the element size and orientation, approximate diagonal dominance may be achieved if the A^{22} terms are greater than the A^{33} terms. As with the boundary elements, this is achieved in practice by incorporation of the following algorithm into the interative solution for the displacement discontinuity components.

(1) For the softer subregion, estimate normal and shear stresses at the interface.

(2) Use these stresses as specified boundary conditions for the stiffer subregion.

(3) For the stiffer subregion, estimate normal and shear displacements at the interface.

(4) Use these displacements as specified boundary conditions for the softer subregion.

Crouch (1976) describes how the displacement discontinuity element may be used to model solid or mined seam elements, mined seam elements which have subsequently been back-filled or fault elements which have failed in shear or tension. These features may be incorporated into the interfaces described above in the same manner as described by Crouch. This is not discussed further here.

It has been found that the rate of convergence of the equations in (38) is about half that for homogeneous problems and that an over-relaxation factor greater than about 1,15 tends to diverge. It is also not possible to use this algorithm for non-homogeneous problems in which a stiffer subregion is completely enclosed within a softer subregion.

The alterations required to the programme MINAP are minimal and a wide range of non-homogenous problems may be solved without violating the restriction imposed above.

CHAPTER 7   PROGRAMME VALIDATION AND NUMERICAL ACCURACY

7.1   Programme BEM

The BEM programme was tested using a homogeneous unit cube under uniaxial tension. The following tests were run:

12   Triangular Elements
24   Triangular Elements
24   Square Elements
96   Triangular Elements

The case with 12 triangular elements was the same as that used by Cruse (1969) (See Fig 7.1). Results from these tests are summarized in Table 7.1. For the 12 triangular element test, a combination of 21 and 42 point integration formulae were used and the results of Cruse (1969) are given for comparison of the numerical and analytical integration of the influence coefficients.

TABLE 7.1:   UNIT CUBE UNDER UNIAXIAL TENSION

12 Elements	Exact	BEM	Cruse (1969)
Reactions of fixed surfaces	1.0000	1.0000	1.000
	1.0000	0.9994	1.000
	0.0000	0.0007	0.000
Maximum axial displacement	1.0000	1.022	1.025
Maximum transverse displacement	1.0000	1.095	1.097
Internal points:			
σ_{11} (.4,.4,.4)	1.000	1.019	1.030
σ_{33} (.4,.4,.4)	0.000	-0.068	-0.074
σ_{13} (.4,.4,.4)	0.000	0.000	-0.010
σ_{12} (.4,.4,.4)	0.000	0.033	0.021
σ_{11} (.4,.4,.6)	1.000	1.020	$-$
σ_{11} (.6,.6,.6)	1.000	1.023	1.028
σ_{23} (.6,.6,.6)	0.000	-0.077	-0.077
σ_{13} (.6,.6,.6)	0.000	0.010	0.012
σ_{23} (.6,.6,.6)	0.000	-0.034	-0.034

NORMAL LOADING OF 1 UNIT.

(1,1,1)

Z

(0,0,1)

NORMAL
DISPLACEMENT=0.

NORMAL
DISPLACEMENT = 0

Y

TRACTION
FREE
SURFACE.

TRACTION
FREE
SURFACE.

X

(0,0,0)   (1,0,0)

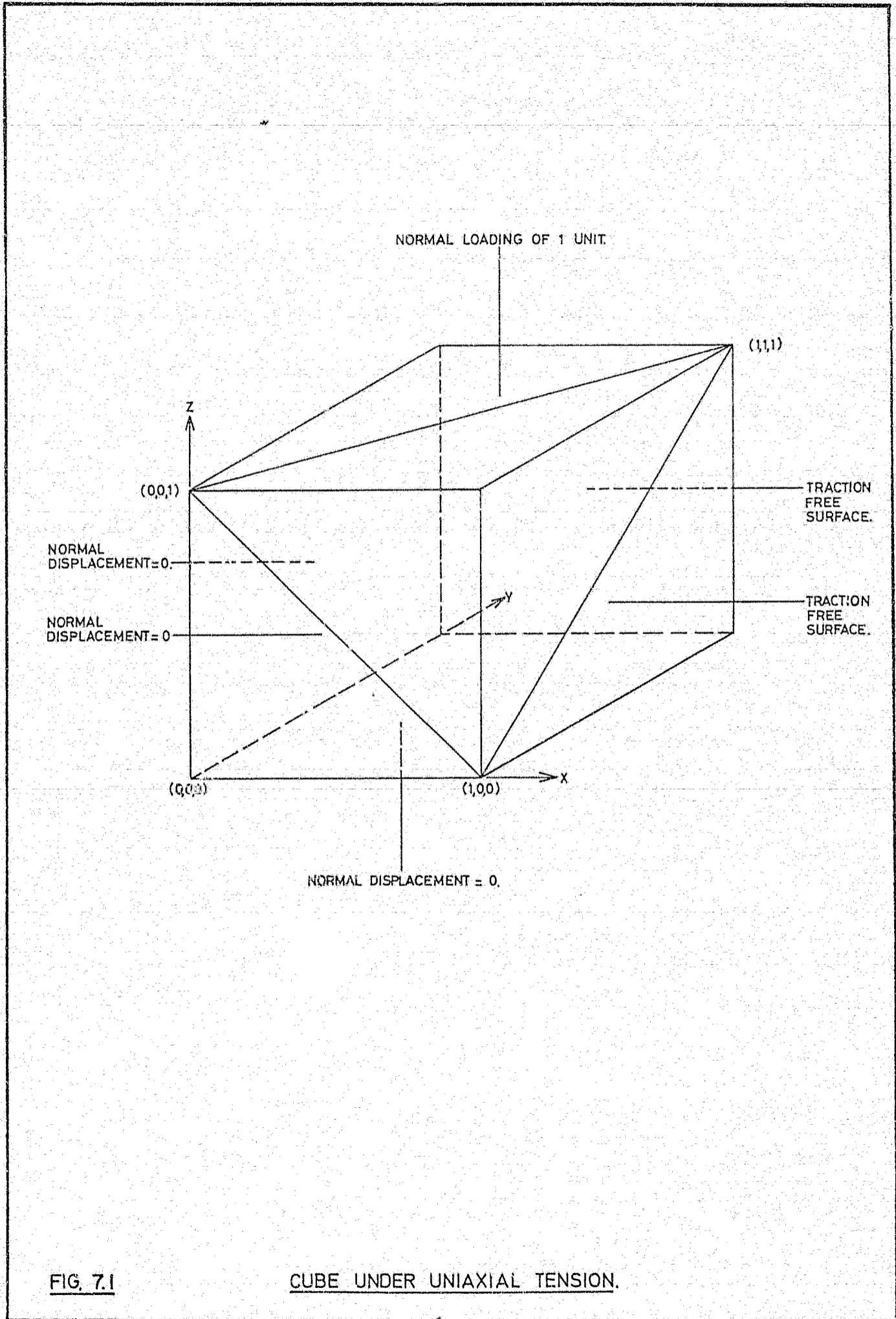NORMAL DISPLACEMENT = 0.

FIG. 7.1   CUBE UNDER UNIAXIAL TENSION.

From these results and similar results from the 24 and 96 element cubes (Table 7.2) it was concluded that the boundary element method programme BEM was working for homogeneous bodies at least. Lumping was used in the 96 element run without seriously affecting the accuracy. As no analytic solution with which to test the programme for non-homogeneous problems was available, the test case of two unit cubes under uniaxial tension, in which one of the loaded ends was rigid, was used (Fig 7.2). Each cube consisted of 12 elements. Answers appeared reasonable when compared with expected answers (Table 7.3).

TABLE 7.2: UNIT CUBE UNDER UNIAXIAL TENSION MODELLED WITH 24 OR 96 ELEMENTS

	Exact	24 square elements	96 elements	96 with lumping
Reactions t_1	1.0000	1.0016	1.010	1.014
t_3	0.0000	0.0042	0.043	0.054
Maximum Axial Displacement	1.0000	1.017	1.014	1.013
Maximum Transverse Displacement	0.300	0.326	0.327	0.332
Internal stresses and displacements				
σ_{11} (0.4,0.4,0.4)	1.000	0.985	0.996	0.993
σ_{33}	0.0000	−0.015	0.011	−0.013
σ_{13}	0.0000	−0.010	−0.0009	0.0019
σ_{23}	0.0000	−0.0091	−0.0013	−0.0054
u_1	0.4000	0.411	0.4064	0.4042

$E_1 = 1,0 \, MPa.$
$V_1 = 0,2.$

$E_2 = 0,5 \, MPa.$
$V_2 = 0,3.$

1MPa.

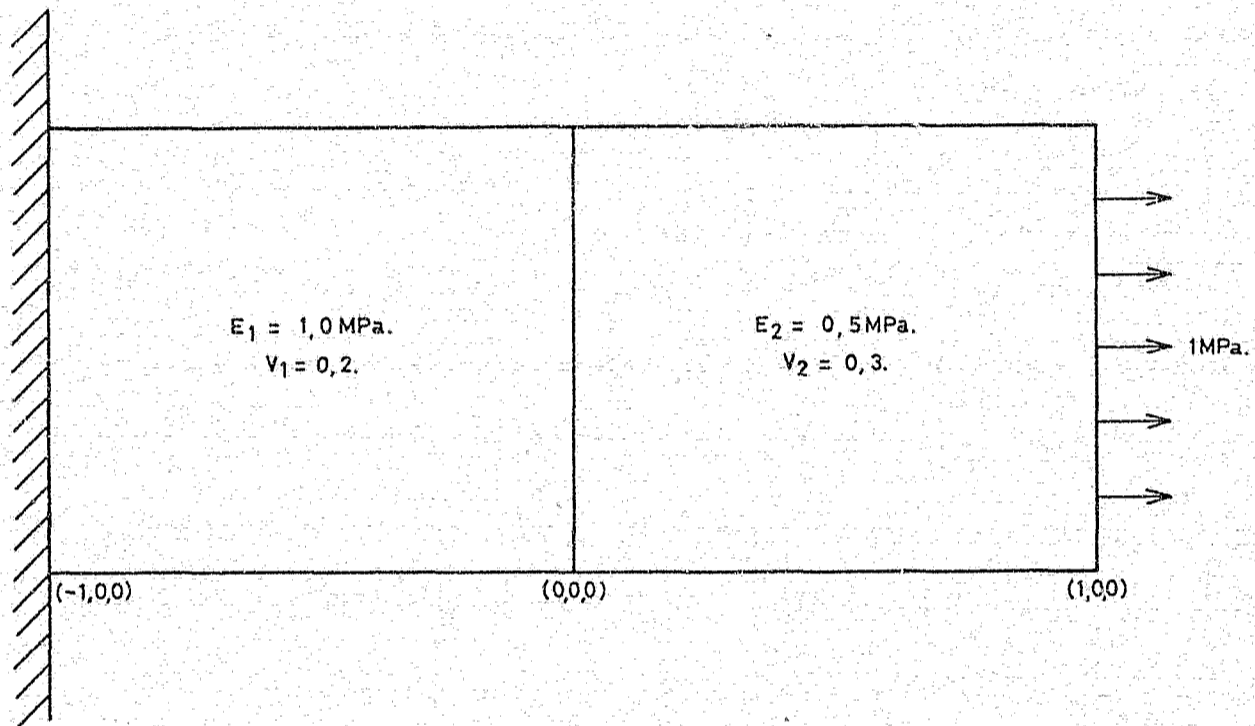$(-1,0,0)$ $(0,0,0)$ $(1,0,0)$

FIG. 7.2   TWO DIFFERENT CUBES UNDER UNIAXIAL TENSION.

TABLE 7.3: RESULTS FOR TWO JOINED CUBES UNDER UNIAXIAL COMPRESSION

	Expected	BEM (42+7 point integration)
Reaction at fixed end	1.000	0.989
	1.000	0.990
	..	-0.702
Reaction at interface	1.000	0.997
	1.000	0.997
Maximum axial displacement	3.000	3.041
Axial displacement at interface	1.000	1.005
Maximum transverse displacement in first cube	0.1 0.15	0.135
Maximum transverse displacement in second cube	0.3	0.333
Internal stresses and displacements		
$\sigma_{11}(0.4,0.4,0.4)$	1.000	1.038
$\sigma_{11}(-0.4,0.4,0.4)$	1.000	0.993
$u_1 (0.4,0.4,0.4)$	1.800	1.785
$u_1 (-0.4,0.4,0.4)$	0.600	0.602
$\sigma_{11}(0.6,0.6,0.6)$	1.000	1.01
$\sigma_{11}(-0.6,-0.6,-0.6)$	1.000	1.011

The effect of lumping and integration accuracy on accuracy and running time was also checked against two-dimensional solutions obtained with the displacement discontinuity programme MINAP. 116 elements were used to represent one eighth of a rectangular tunnel measuring 34 m x 3,2 m x 6 m (the height being 3,6m). The vertical stress was 60 MPa and the horizontal streses 30 MPa each (Fig 7.3). Element sizes were graded further from the tunnel centre where 8 elements were used to span half the hangingwall and 8 for half the sidewall. Table 7.4 shows a comparison of displacements for two MINAP and 4 boundary element runs (the displacements represent vertical displacements along the hangingwall section of the tunnel). Details of the integration constants and running times are given in Table 7.5.
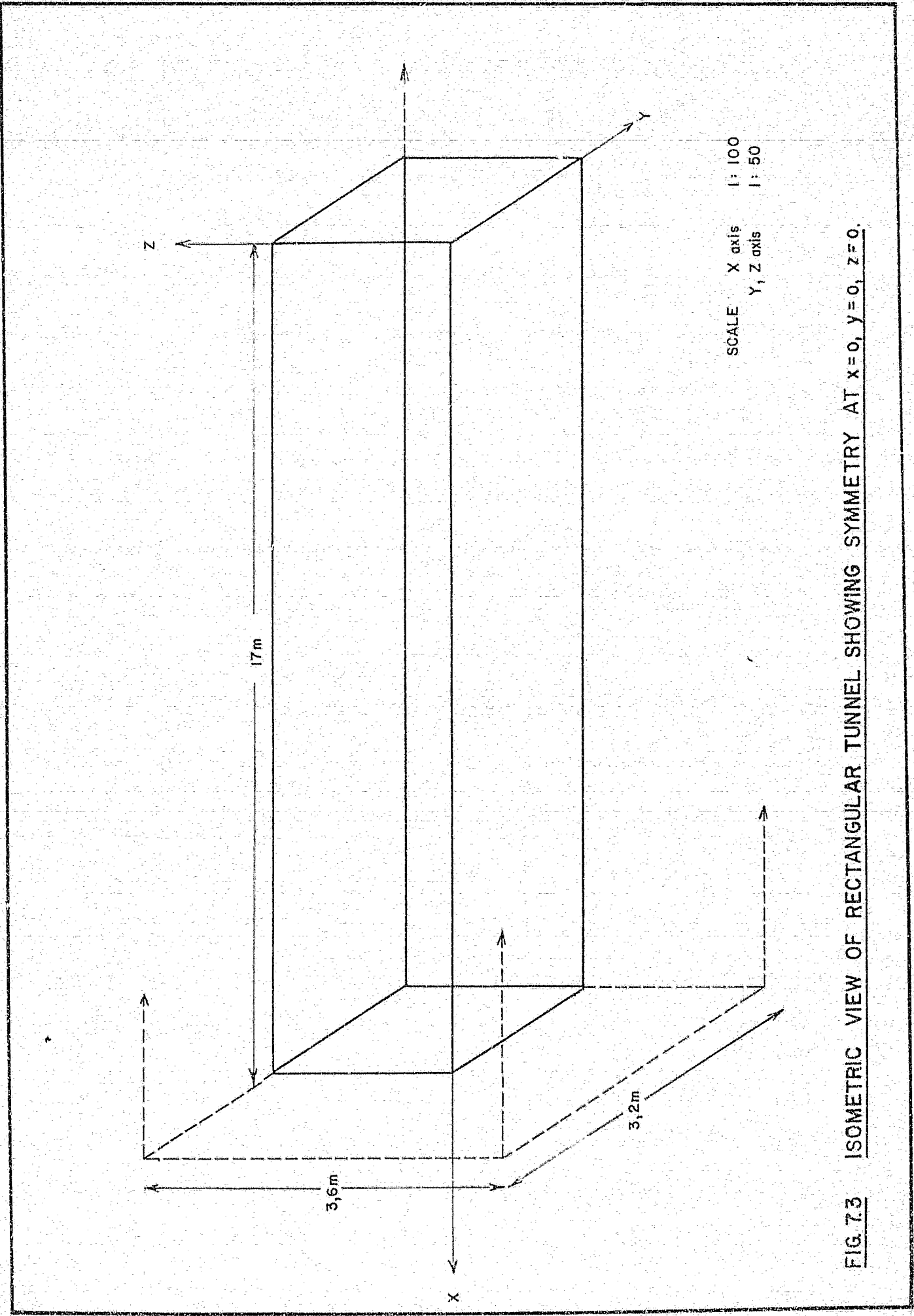
SCALE   X axis   1: 100
         Y, Z axis   1: 50

17m

Z

Y

X

3,6m

3,2m

FIG. 7.3   ISOMETRIC VIEW OF RECTANGULAR TUNNEL SHOWING SYMMETRY AT x=0, y=0, z=0.

TABLE 7.4: COMPARISON OF BOUNDARY DISPLACEMENTS FOR RECTANGULAR
TUNNEL

Point	48 element MINAP	16 element MINAP	Run 1	Run 2	Run 3	Run 4
1	,00344	,00348	,00342	,00341	,00340	,00337
2	,00340	,00344	,00338	,00337	,00336	,00332
3	,00332	,00336	,00330	,00329	,00327	,00324
4	,00319	,00324	,00317	,00316	,00315	,00311
5	,00301	,00306	,00299	,00299	,00.97	,00294
6	,00276	,00282	,00274	,00274	,00274	,00267
7	,00242	,00249	,00240	,00240	,00238	,00236
8	,00190	,00202	,00189	,00189	,00187	,00185

Table 7.6 shows comparisons of stresses at interior points. The x-y co-ordinates are such that the hangingwall lies at $y = 1,8$ and the sidewall at $x = 1,6$. The tables clearly show the high order of integration required to obtain reasonable results for stresses at interior points. Such accurate integration is unnecessary when solving for surface displacements and tractions and the time savings obtained by lumping and variable integration accuracy are clearly demonstrated by Table 7.5.

TABLE 7.5: RUNNING TIMES AND INTEGRATION SCHEME COMPARISON

Item	Run 1	Run 2	Run 3	Run 4
42 Point Transition Ratio	1,2	1,2	1,0	0,3
21 Point Transition Ratio	2,5	2,5	2,5	0,7
7 Point Transition Ratio	5	5	2	2
3 Point Transition Ratio	10	10	5	5
Lumping Transition Ratio	9999	12	12	4,5
Time for influence Coefficients	197 mins	131 mins	122 mins	82 mins
Time for Solution (12 Iterations)	24,6 mins	17,4 mins	7,1 mins	15,4 mins
Time for Interior Point (Average)	3,6 mins	1,8 mins	1,7 mins	0,95 mins
Total time (with 41 Int. Points)	369 mins	222 mins	208 mins	160 mins
Disk Storage (Blocks)	995	604	604	468

TABLE 7.6:   COMPARISON OF STRESSES AT INTERIOR POINTS

RUN	x	y	σ_x	σ_y	σ_{xy}	x	y	σ_x	σ_y	σ_{xy}
MINAP1	0,4	2,0	13,5	0,49	-1,74	2,2	1,2	13,3	88,3	-17,2
MINAP2	0,4	2,0	13,9	0,56	-1,83	2,2	1,2	12,5	88,9	-16,8
BEM 1	0,4	2,0	12,9	-1,59	-0,45	2,2	1,2	12,3	87,2	-16,6
BEM 2	0,4	2,0	12,9	-1,47	-0,40	2,2	1,2	12,3	87,0	-16,5
BEM 3	0,4	2,0	4,0	56,10	-2,76	2,2	1,2	13,3	87,0	-16,2
BEM 4	0,4	2,0	4,5	55,80	-2,60	2,2	1,2	13,7	86,9	-15,8
BEM 4*	0,4	2,0	12,9	0,70	-0,90	2,2	1,2	13,0	86,9	-16,5

* Using same integration constants for interior points as in BEM 1 run.

7.2 Mixed boundary element programme MBEM

Before combining the boundary elements with displacement discontin-
uity elements, a test was done to compare the two methods. The dis-
placement discontinuity programme RIDE used is described elsewhere
(Starfield and Crouch 1973, Diering 1977). A square flat planar
tabular excavation of dimensions 80 m x 80 m subjected to a normal
load of 60 MPa was used as the test case and 98 boundary elements
with dimensions ranging from 40 m square to 10 m square were used.
Two displacement discontinuity runs were done with 64 10 m square
elements and 16 20 m square elements. The region discretized for the
boundary element run was 160 m x 160 m square. Tables 9 and 10 show
a comparison of (hangingwall/footwall convergence) and interior
stresses and displacements (in the hangingwall).

TABLE 10:   COMPARISON OF CLOSURES - PROGRAMMES BEM AND RIDE

Point	BEM	RIDE (10m)	RIDE (20m)
1	7,9	8,5	14,5
2	14,4	15,0	14,5
3	18,4	19,0	22,0
4	20,3	21,0	22,0
5	19,3	20,0	21,7

TABLE 7.8: COMPARISON OF INTERIOR STRESSES AND DISPLACEMENTS
PROGRAMMES BEM AND RIDE

Distance to excavation (m)	Vertical displacement		Minimum principle stress	
	BEM	RIDE	BEM	RIDE (20m)
50	−4,7	−6,2	15,9	13,8
30	−8,2	−9,4	9,2	7,7
10	−14,2	−15,20	−0,5	−20,8

The discrepancy in displacements 50 m above the excavation probably
arises from the limited size of the boundary element mesh while the
large tensile stress given by the displacement discontinuity method
10 m in the hangingwall is as a result of the 1 point integration
formula used in evaluating the stress. The otherwise good agreement
between the displacements prompted the combination of the two element
types. Running times were:

BEM   100 minute   (294 degrees of freedom)
RIDE   7 minute   (64 degrees of freedom)

In modelling the excavation with boundary elements, it was possible
to discretize only the hangingwall and surrounding solid areas of the
excavation. If hangingwall and footwall movements were unequal, then
twice as many boundary elements would have been required. The great
advantages of the displacement discontinuity elements over the boun-
dary elements for this type of problem are evident.

A direct verification of the MBEM programme appeared very difficult
but was not necessary since all of the programming logic appeared in
one or other of the programmes RIDE or BEM. A number of direct test
examples have been run and answers from these tests have appeared to
be reasonable. One example is given here - a 4 x 4 array of displace-
ment discontinuity elements. As the depth S increases the dis-
placements of the boundary element tend to zero while the closures in
the displacement discontinuity elements tend towards those of an
independent RIDE run. When the depth S is small, then the hanging-
wall movements become significantly greater than the footwall move-

ments (as has been demonstrated by Crouch (1976) in two dimensions).
When the depth $\overline{z}$ becomes less than about 0,75 of the maximum ele-
ment width, then numerical convergence is lost. As the constant dis-
placement and constant traction assumptions for each element are no
longer valid in this case it is fortunate that the programme automat-
ically rejects such ill-conditioned or badly specified problems.
Indeed, the accuracy achieved in any problem, appears to be strongly
related to the rate of convergence of the numerical solution. There
are of course many exceptions to this general rule.

A second method of testing the programme was to vary all of the inte-
gration parameters to check the dependence of the solutions upon the
accuracy of numerical integration.

CHAPTER 8 PROGRAMMING CONSIDERATIONS

The size of a programme is governed by the number of programming steps making up the programme and by the amount of data required or used by the programme.

8.1 Programme structure

The core requirements of a programme are easily reduced by using programme overlays or "swaps". Only that portion of the programme which is in use is held in main memory. Provided the programme is well structured, the amount of swapping of programmes in and out of main memory is minimal and results in negligable increase in total running time. Fortunately, boundary and finite element formulations are well structured and the BEM and MBEM programmes were easily divided into the following swaps.

   (i)   Control programme
  (ii)   Input and data checking
 (iii)   Calculation of influence coefficients
  (iv)   Iterative solution for unknown displacements and tractions
   (v)   Output of displacements and tractions
  (vi)   Calculation of stresses and displacements at specified points

It is possible to stop or start the programme at any stage. Thus, for example, it is possible to store the displacement and traction solutions for a number of runs (iv) while overwriting the very large influence coefficient file (iii), if necessary for successive runs. Stresses and displacements may subsequently be calculated at any point for any of the displacement/traction solutions. A typical application of the above procedure arises when a number of different geometries for a problem are studied. After the initial analysis, it becomes necessary to determine stresses and displacements at a few additional points without repeating the entire analysis. This is easily achieved with the above programme structuring.

8.2 Data storage

8.2.1 The influence coefficient file (ICF)

The file containing the influence coefficients (the ICF) can easily become very large. For example, a problem containing 1 000 elements (in which the lumping mechanism was not used to reduce the number of influence coefficients, would require about 36 M bytes.

In designing the programme, it was decided to use sequential access for the ICF. That is to say, the influence coefficients are calculated in precisely the same order as needed during the iterative solution stage. The use of sequential access for the ICF makes it possible to store the ICF on tape. This will be done shortly, and it is expected that the increase in running time will be more than offset by the reduced cost of cheaper peripheral storage.

Access time to the ICF is reduced by retaining in core a fairly large buffer array (8 k byte in the present versions). This buffer array is also accessed sequentially and a disk/tape transfer is only required every 2 000 coefficients (1 coefficient = 4 bytes).

All access to the ICF is controlled by one small subroutine so that the programmes are not too machine specific.

8.2.2 Storage of lump elements

All the information for the elements of any one lump is stored on two disk blocks of 512 bytes each. This information includes displacements, tractions, direction cosines, areas and codes. The nodal co-ordinates which are used by more than one lump in many cases are retained in main memory.

Since it is never necessary to retain in main memory the detailed information of more than two lump elements at any one time, the two lump elements are referred to as a receiving and an emitting lump element. Each has assigned to it a labelled common block of 512 words. It is thus a simple matter to read or write the information for all the elements within a lump to or from disk.

8.3 Programme listings

A complete listing of programme BEM is given in Appendix 2 while partial listings of programmes MBEM and MINAPH are given in Appendix 3 and 4. A partial listing of MBEM is given to avoid repetition since numerous subroutines are either common to BEM and MBEM or at least similar to one another.

A partial listing of MINAPH is given because the original programme was developed by Crouch (1976). Only those sections which were changed to facilitate modelling of non-homogenous problems are given.

CHAPTER 9   EXAMPLES OF PRACTICAL APPLICATIONS

Before describing some of the practical applications of BEM and MBEM, it is useful to briefly summarise some of the uncertainties which accompany a typical stress analysis problem in rock mechanics.   In addition, a number of useful rules of thumb have evolved from the use of these programmes.

The loading for a problem arises primarily from the primitive or in situ stresses which are present in the rock mass before mining commences.   It is possible to measure these stresses with reasonable accuracy, (Gay, 1975) but the presence of dykes, faults etc can result in a fairly irregular stress distribution in the rock mass even before any mining commences.   A more usual approach is to assume that the overburden stresses increase linearly with depth below surface and that horizontal stresses are a constant fraction of the vertical stress. Gay (1975) shows how the horizontal to vertical stress ratio varies with depth on average in Southern Africa.

The excavation geometry for a typical problem is usually very complex so that a number of simplifying assumptions have to be made.   Usually, service excavations are much smaller than the production excavations, so that only the latter are modelled. Sometimes the extent of mining is such that it is not possible to model all the production excavations.   Typical examples of this occur in the Witwatersrand gold fields where mining is more or less continuous for distances exceeding twenty five kilometers.

The geology of most problems is usually complex and is also usually based on a number of boreholes.   It is practical therefore only to consider major geological horizons with significantly different material properties.

The material properties are seldom known with any great degree of certainty.   Apart from material anisotropies which are difficult to measure, a number of other problems arise in assessing suitable material properties.   Elastic moduli and material strength are usually determined from small specimen tests.   It is known that actual large scale properties

Author Diering J A C
Name of thesis Further developments of the boundary element method with applications in mining 1981